

A Pariser-Parr-Pople Model Based Study of Optoelectronic Properties of Phenacenes

Deepak Kumar Rai* and Alok Shukla†

*Department of Physics, Indian Institute of
Technology Bombay, Powai, Mumbai 400076, India*

Abstract

In this paper we present a computational study of linear optical absorption in phenacene class of polyaromatic hydrocarbons. For the purpose, we have employed a correlated-electron methodology based upon configuration-interaction (CI) approach, and the Pariser-Parr-Pople (PPP) π -electron model Hamiltonian. The molecules studied range from the smallest one with three phenyl rings (phenanthrene), to the largest one with nine phenyl rings. These structures can also be seen as finite-sized hydrogen-passivated armchair graphene nanoribbons of increasing lengths. Our CI calculations reveal that the electron-correlation effects have a profound influence not just on the peak locations, but also on the relative intensity profile of the computed spectra. We also compare our phenacene results with isomeric oligo-acenes, and find that in all the cases former have a wider optical gap than the latter. Available experiments based upon optical absorption and electron-energy-loss-spectroscopy (EELS) are in very good agreement with our results.

I. INTRODUCTION

Over last several decades, polycyclic aromatic hydrocarbons (PAHs) have been studied extensively using theoretical and experimental methods, because of their importance in several fields such as physics, chemistry, environmental science, astrophysics and biology.¹⁻⁴ PAHs, with a planar structure, are π -conjugated systems, known for strong response to external fields, thus with potentially numerous device applications.^{5,6} Oligoacenes, particularly tetracene and pentacene are among the most studied PAHs because of their possible applications in the field of optoelectronic devices, particularly light-emitting diodes, and photovoltaic cells.^{7,8} Phenacene oligomers, which are nothing but the isomers of oligo-acenes of the same length, have also been found to be very useful in the field of the device application, particularly in fabrication of organic field-effect transistors (FETs).^{5,9-14} Furthermore, it was reported that one of the phenacene oligomers, namely picene, exhibits high-temperature superconducting behavior when doped by alkali metals.¹⁵ Phenacenes are similar to oligoacenes in that both are composed of fused benzene rings, while differing from each other in the way the fused rings are arranged. In oligoacenes, the fused rings are arranged in a straight manner leading to D_{2h} symmetry, while in phenacenes, they are arranged in a zigzag manner resulting in the point group is C_{2h} if the number of rings is even, and C_{2v} for odd number of rings. A phenacene oligomer with n fused rings is called $[n]$ phenacene, and it is obvious that the minimum possible value for $n = 3$. For $3 \leq n \leq 6$, phenacene oligomers are named phenanthrene ($n = 3$), chrysene ($n = 4$), picene ($n = 5$), and fulminene ($n = 6$), while for $n > 6$, they are referred as $[n]$ phenacene.

Motivated by potential device applications of phenacenes, in this work we undertake a systematic computational study of their electronic structure, low-lying excited states, and linear optical response. Such a study is necessary not just for understanding the optical properties of individual oligomers, but also for obtaining insights into the transport properties of these materials in the crystalline phase, which consists of nothing but individual molecules held together by van-der-Waals binding. Given the fact that the phenacenes are π -electron systems, we have employed our Pariser-Parr-Pople model based electron-correlated methodology for this study¹⁶. The oligomers studied in this work range from phenanthrene to $[9]$ phenacene, and our results are found to be in excellent agreement with the experimental measurements, wherever available. Because $[n]$ phenacene is isomeric with acene- n , we also

compare present results with the ones obtained for polyacenes in an earlier work from our group,¹⁷ with the aim of understanding the role of geometry on the optical properties of these materials. We find that for each value of n considered in this work, optical absorption spectra of two classes of materials are qualitatively different, and that the optical gap of $[n]$ phenacene is significantly larger than that of acene- n . This suggests that the optical absorption spectroscopy can be used to distinguish between isomeric phenacenes and acenes.

The remainder of the paper is structured as follows. In Section II we present schematic diagrams of phenacenes, and discuss their point group symmetries, and related consequences. This is followed in Section III by a brief discussion of the theoretical methodology adopted in this work. Next, in Section IV we present and discuss the results of our calculations, followed by conclusions and outlook in Section V.

II. MOLECULAR STRUCTURE AND POINT GROUP SYMMETRY

In Fig. 1, we present the schematic diagrams of $[n]$ phenacenes considered in this work, along with their point group symmetries. We take the conjugation direction (long axis) to be x axis, and the perpendicular direction (short axis) to be y axis, so that all oligomers lie in the $x - y$ plane, with a uniform C-C bond length of 1.4 Å, and all the edge carbon atoms are assumed to be passivated by hydrogen atoms. $[n]$ phenacene, just like acene- n , has $4n + 2$ carbon atoms, as also the same number of π -electrons. The point group symmetry of phenanthrene (14 carbon atoms), picene (22 carbon atoms), [7]phenacene (30 carbon atoms), and [9]phenacene (38 carbon atoms) is C_{2v} , with 1^1A_1 being the ground state. On the other hand, the point group symmetry of chrysene (18 carbon atoms) fulminene (26 carbon atoms) and [8]phenacene (34 carbon atoms) is C_{2h} , with 1^1A_g being the ground state. As per electric-dipole selection rules, the symmetries of the one-photon excited states are 1^1A_1 (y polarized) and 1^1B_1 (x polarized) for C_{2v} molecules, and 1^1B_u (xy -polarized) for C_{2h} molecules.

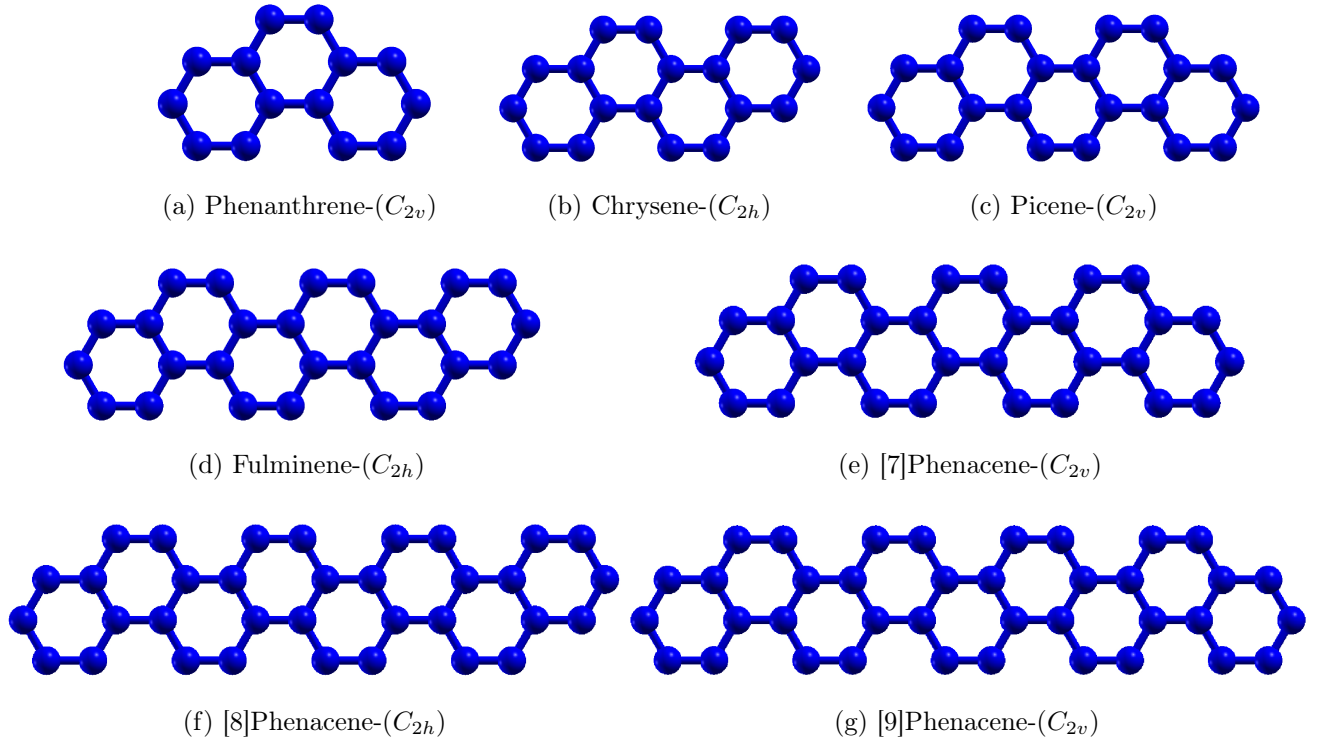


Figure 1: Schematic diagrams of phenacenes, along with their point-group symmetries.

III. THEORETICAL METHODOLOGY

As described in the previous section, the molecules considered here are π -conjugated systems, and, therefore, in this work we adopt Pariser-Parr-Pople (PPP) model Hamiltonian,^{18,19} reviewed in our earlier work¹⁶

$$\begin{aligned}
 H = & -\sum_{i,j,\sigma} t_{ij} \left(c_{i\sigma}^\dagger c_{j\sigma} + c_{j\sigma}^\dagger c_{i\sigma} \right) + U \sum_i n_{i\uparrow} n_{i\downarrow} \\
 & + \sum_{i < j} V_{ij} (n_i - 1)(n_j - 1),
 \end{aligned} \tag{1}$$

where $c_{i\sigma}^\dagger$ ($c_{i\sigma}$) denotes creation (annihilation) operators corresponding to an electron of spin σ in a p_z orbital, located on the i -th carbon atom, while the total number of electrons on the atom is indicated by the number operator $n_i = \sum_\sigma c_{i\sigma}^\dagger c_{i\sigma}$. In Eq. 1, the first term denotes the one-electron hoppings connecting i -th and j -th atoms, quantified by matrix

elements t_{ij} . It is assumed that the hopping connects only the nearest-neighbor carbon atoms, with the matrix element $t_0 = 2.4$ eV, consistent with our earlier calculations on conjugated polymers,^{17,20–25} polyaromatic hydrocarbons,^{26,27} and graphene quantum dots.^{28,29} The remaining two terms in Eq. 1 represent the electron-electron repulsion terms, with the parameters U , and V_{ij} , denoting the on-site, and the long-range Coulomb interactions, respectively. The distance-dependent Coulomb parameters V_{ij} are computed according to the Ohno relationship³⁰

$$V_{ij} = U/\kappa_{i,j}(1 + 0.6117R_{i,j}^2)^{1/2}, \quad (2)$$

where $\kappa_{i,j}$ is the dielectric constant of the system, included to take into account the screening effects, and $R_{i,j}$ is the distance (in Å) between the i th and j th carbon atoms. In the present set of calculations we have used two sets of Coulomb parameters: (a) the “screened parameters”³¹ with $U = 8.0$ eV, $\kappa_{i,j} = 2.0(i \neq j)$, and $\kappa_{i,i} = 1.0$, and (b) the “standard parameters” with $U = 11.13$ eV and $\kappa_{i,j} = 1.0$.

The calculations are initiated by performing restricted Hartree-Fock (RHF) calculations for the closed-shell singlet ground states of phenacenes considered here, using a computer program developed in our group.³² The molecular orbitals (MOs) obtained from the RHF calculations form a single-particle basis set used to transform the PPP Hamiltonian from the site representation, to the MO representation. Subsequently, correlated-electron calculations using the configuration interaction (CI) approach are performed. The level of the CI calculations is decided by the size of the molecule under consideration. For smaller molecules, one can use full-CI (FCI) or quadruple-CI (QCI) approaches, however, for the larger systems only the multi-reference singles-doubles configuration interaction (MRSDCI) approach is tractable. In the MRSDCI calculations, the CI expansion is generated by exciting up to two electrons, from a chosen list of reference configurations, to the unoccupied MOs.^{33,34} The reference configurations included in the MRSDCI method depend upon the states in consideration, which can be the ground state, or optically excited states.^{17,20–25,28}

Once the many-body wave functions and the energies of the ground and the excited states are obtained from the CI calculations, we compute the optical absorption cross-section $\sigma(\omega)$, according to the formula

$$\sigma(\omega) = 4\pi\alpha \sum_i \frac{\omega_{i0} |\langle i | \hat{e} \cdot \mathbf{r} | 0 \rangle|^2 \gamma^2}{(\omega_{i0} - \omega)^2 + \gamma^2}. \quad (3)$$

In the equation above, $\hat{\mathbf{e}}$ represents the polarization direction of the incident light, ω denotes its frequency, \mathbf{r} is the electronic position operator, indices 0 and i represent, respectively, the ground and excited states, ω_{i0} is the frequency difference between those states, α denotes the fine structure constant, and γ is the assumed universal line width. The summation over i , in principle, is an infinite sum, which, in practice, is restricted to those dipole-connected excited states, whose excitation energies are within a certain cutoff, taken to be 10 eV in these calculations.

IV. RESULTS AND DISCUSSIONS

In this section we present the calculated linear optical absorption spectra and optical gaps of $[n]$ phenacenes, and compare our results with the experiments, wherever available. Our calculations were performed using both the tight-binding (TB) model, as well as PPP model using the CI approach, and we find that our PPP-CI results are in much better agreement with experiments.

A. Tight-Binding Model Results

Because the tight-binding (TB) model is an independent electron approach, therefore, results obtained using it will help us understand the influence of electron correlation effects, when compared with the results computed using the PPP-model. We first present and discuss the optical absorption spectra obtained using the TB-model, followed by a discussion of the optical gaps.

1. Linear Optical absorption spectra

In Fig. 2, we present the optical absorption spectra of $[n]$ phenacenes obtained using the TB method. An examination of the spectra reveals the following trends: (a) With the increasing lengths of the oligomers, absorption spectra are red shifted, consistent with the phenomenon of the quantum confinement effect. (b) The first peak for all the oligomers corresponds to the excitation of an electron from HOMO (H) to LUMO (L). It corresponds to transition to 1^1B_1 state via absorption of a photon polarized along the length

(x -direction) of the C_{2v} symmetric oligomers. For C_{2h} symmetry, the first peak is due to 1^1B_u state, reached via absorption of an xy -polarized photon, with the x -component much stronger than the y -component. (c) The maximum intensity peak is the first peak for all the oligomers, except for chrysene for which the second peak is the most intense one, and it is due to $|H \rightarrow L + 1\rangle + c.c.$ excitation, where $c.c.$ denotes the corresponding charge-conjugated configuration.

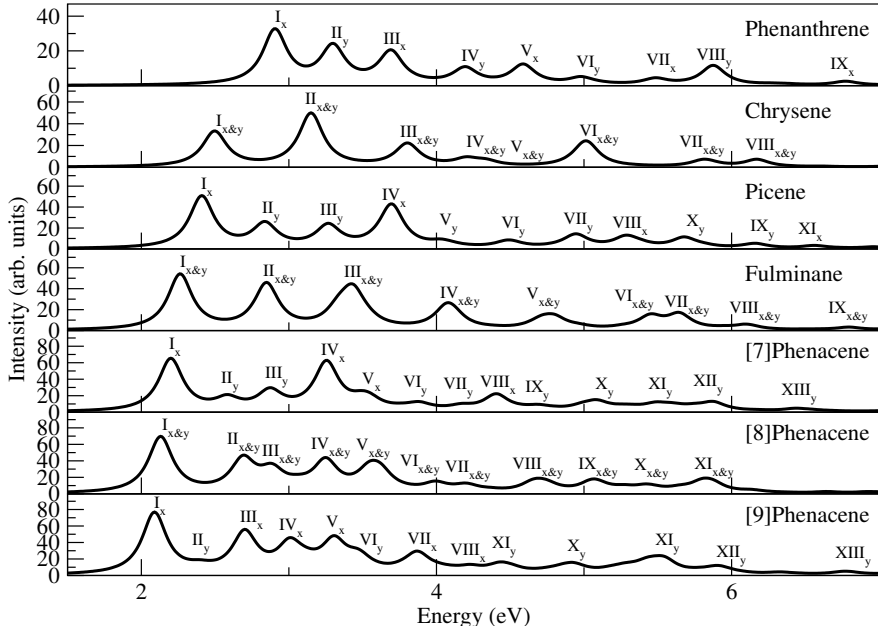


Figure 2: Optical absorption spectra of $[n]$ phenacenes ($n = 3 - 9$), computed using the TB model. The spectra have been broadened using a uniform line-width of 0.1 eV.

2. Optical Gap

The locations of the first absorption peaks of $[n]$ phenacenes, i.e. their optical gaps, computed using various approaches are presented in Table I, where they are also compared to the experimental results. The following conclusions can be drawn from this table: (a) Independent of the Hamiltonian, gaps decrease with the increasing length of $[n]$ phenacene, (b) the gaps obtained for $[n]$ phenacenes using the TB method are much smaller compared to the corresponding experimental, as well as PPP-CI values, (c) the gaps obtained using the PPP-CI method, employing screened parameters, are in very good agreement with the experimental values.

Table I: Locations of the first absorption peaks for increasing length of $[n]$ phenacenes, obtained using the TB and the PPP-CI approaches. For the PPP-CI calculations, both the screened (Scr.) and the standard (Std.) parameters are employed.

System	Optical gap (eV)				
	TB Model	PPP-CI		Experimental	Theory (other authors)
		Scr.	Std.		
Phenanthrene	2.90	4.31	4.26	4.09 ³⁵ , 4.17 ¹² , 4.24 ¹ , 4.24 ³⁸ , 4.25 ³⁹ , 4.36 ⁴⁰ ,	3.91 ³⁶ , 4.19 ³⁷ , 4.31 ³⁶ , 4.34 ³⁶ , 4.36 ⁴¹ , 4.53 ⁴² , 4.60 ⁴³ , 4.67 ³⁷ ,
Chrysene	2.49	3.86	3.96	3.74 ³⁵ , 3.84 ¹² , 3.87 ⁴⁴ , 3.89 ¹ , 3.89 ^{38,45} ,	3.40 ³⁶ , 3.43 ⁴² , 3.73 ³⁷ , 3.82 ³⁶ , 3.90 ⁴⁶ , 3.92 ³⁶ , 4.13 ⁴¹ , 4.21 ³⁷ , 4.22 ⁴³
Picene	2.40	3.75	3.88	3.76 ^{12,45} , 3.77 ¹ , 3.80 ³⁸ , 3.82 ⁴⁷ ,	3.32 ³⁶ , 3.70 ³⁷ , 3.72 ³⁶ , 3.83 ³⁶ , 4.13 ⁴³ , 4.19 ³⁷ ,
Fulminene	2.26	3.34	3.52	3.14 ⁵ , 3.24 ¹² , 3.76 ⁴⁵ ,	3.47 ³⁷ , 4 ³⁷ ,
[7]Phenacene	2.19	3.34	3.68	3.10 ⁵ , 3.60 ⁴⁵ ,	3.50 ³⁷ , 4 ³⁷ ,
[8]Phenacene	2.13	3.11	3.41	3.08 ⁵	—
[9]Phenacene	2.08	3.09	3.46	3.05 ¹¹ ,	—

B. PPP Model Based Optical absorption Spectra

In this section we present the results of our calculations of optical absorption spectra of $[n]$ phenacenes, performed using the PPP-CI approach. Before we discuss our results, we present the dimensions of the CI matrices involved in the calculations, for various irreducible representations of phenacenes.

1. *Dimensions of the CI matrices*

Most accurate results within the CI approach are obtained when the full-CI (FCI) calculations are performed, which involves distributing all electrons, in all available molecule orbitals, in all possible ways, consistent with the symmetries. Therefore, the size of the FCI matrix increases exponentially with the increasing size of the molecule involved, making it feasible only for small molecules. Thus, in this work we were able to perform FCI calculations only on the smallest oligomer, namely phenanthrene. For chrysene and picene we were able to perform QCI calculations. For remaining oligomers, because of their larger sizes, we employed the MRSDCI approach. Even within the truncated CI approaches such as the QCI and the MRSDCI methods, larger-sized CI expansions normally lead to more accurate results. Therefore, in the section, to illustrate the accuracy of our calculations, we present the dimensions of the MRSDCI matrices in Table II.

Table II: Dimension of CI matrices (N_{total}) involved in the calculations of the optical absorption spectra, for different symmetry subspaces of $[n]$ phenacenes.

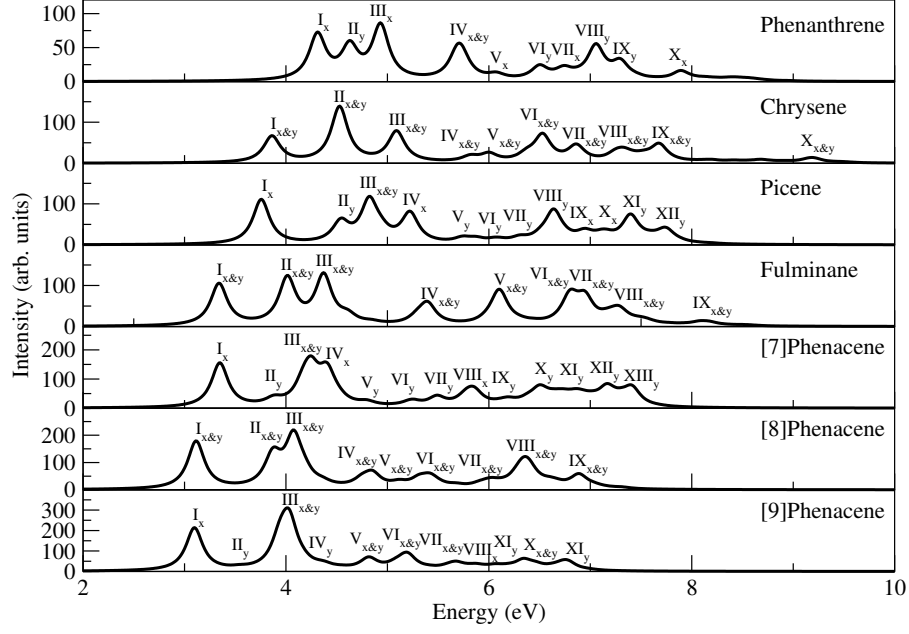
Molecules	N_{total}			
	1A_1	1B_1	1A_g	1B_u
Phenanthrene	1244504 ^a	1239406 ^a	-	-
Chrysene	-	-	386498 ^b	670593 ^b
Picene	2003907 ^b	3416371 ^b	-	-
Fulminene	-	-	7877992 ^b	1053746 ^c
	-	-	7877992 ^b	1300041 ^d
[7]Phenacene	2303318 ^c	5720562 ^c	-	-
	3043013 ^d	2645512 ^d	-	-
[8]Phenacene			377903 ^c	3300974 ^c
			628766 ^b	5223159 ^d
[9]Phenacene	2617790 ^c	3056846 ^c		
	4672916 ^d	5876058 ^d		
FCI ^a method with screened and standard parameters. QCI ^b method with screened and standard parameters. MRSDCI ^c method with screened parameters. MRSDCI ^d method with standard parameters.				

It is obvious from the table that in various calculations N_{total} ranges from 3.6×10^5 to 7.8×10^6 . This implies that our calculations employ large CI expansions, and, therefore, should be fairly accurate, yielding reliable results.

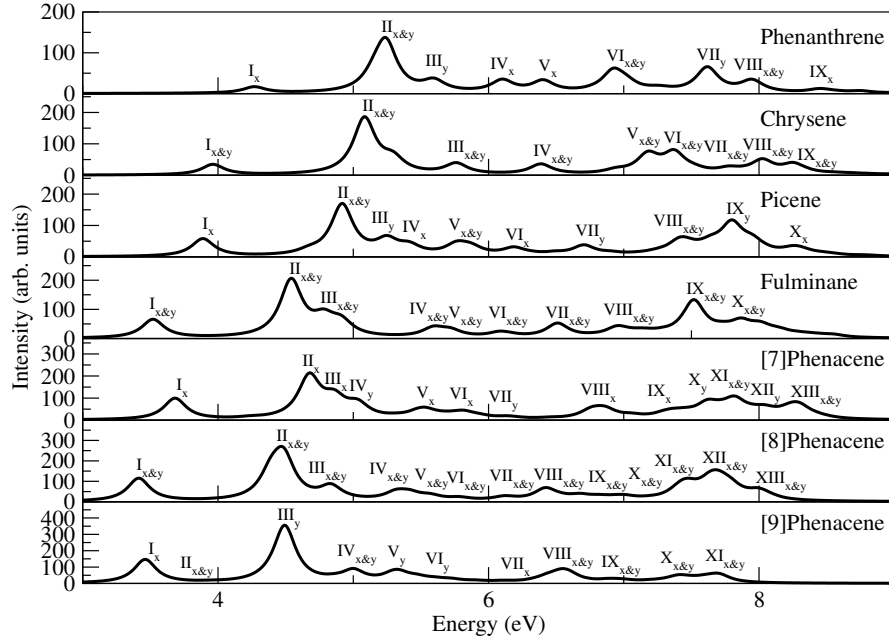
2. Optical absorption spectra

First we discuss the general trends observed in the optical absorption spectra of $[n]$ phenacenes calculated using the PPP-model, and the MRSDCI approach, presented in Fig. 3.

Detailed information related to peaks contributing to the spectra, such as the many-particle wave functions, energies, and transition dipole moment etc. are presented in Tables S1-S14 of Supporting Information. By carefully examining the optical absorption spectra (Fig. 3), we observed the following trends: (a) Similar to the case of TB model, with the



(a) screened parameters



(b) standard parameters

Figure 3: Calculated optical absorption spectra of $[n]$ phenacenes, using the PPP-CI method, by employing screened, as well as standard parameters. The spectra have been broadened with a uniform line-width of 0.1 eV.

increasing length of [n]phenacene, spectra is red-shifted for the screened parameter calculations. For the standard parameters, again the spectra are red-shifted, except for the case of [7]phenacene. (b) the lowest energy absorption in [n]phenacenes corresponds to a dipole forbidden state of symmetry 1A_1 for C_{2v} molecules, and 1B_u for C_{2h} molecules. The wave functions of the corresponding state is dominated by single excitations $|H \rightarrow L + 1\rangle + c.c.$ for oligomers up to [7]phenacene, and $|H \rightarrow L + 2\rangle + c.c.$, for longer oligomers. (c) In all the calculations, the first dipole-allowed peak corresponding to the optical gap is not the most intense one of the spectrum, in contradiction with the TB model results, and in agreement with the experiments. In the screened parameter calculations, the relative intensity of the first peak, as compared to the most intense peak, is much larger than that in the standard parameter calculations. In agreement with the results of TB model, the first peak for the C_{2v} symmetric molecules corresponds to 1^1B_1 state, and for C_{2h} symmetric molecules to 1^1B_u state, and in all the cases the dominating configuration in the many-particle wave function of this state is $|H \rightarrow L\rangle$, single excitation. (d) The maximum intensity peak occurs at higher energies, and the wave functions of the two excited states contributing to it are dominated by single excitations: (i) $|H - 1 \rightarrow L + 1\rangle$ or $|H - 2 \rightarrow L + 2\rangle$, and (ii) $|H \rightarrow L + 1\rangle + c.c.$ or $|H \rightarrow L + 2\rangle + c.c.$, which are the same excitations which contribute to the D.F. state. Next we discuss the optical absorption spectra of the individual phenacenes in detail.

Phenanthrene

Phenanthrene has C_{2v} symmetry, and Klevens *et al.*³⁵, Okamoto *et al.*¹², Clar *et al.*¹, Salama *et al.*³⁹ and Halasinski *et al.*⁴⁰ have reported the measurements of its absorption spectrum. In Fig. 3 (a) and (b), we present our calculated spectra using the screened and standard parameters, respectively, within the PPP-CI approach, and in Table III, we have compared our results on the locations of various peaks with the experiments, and other theoretical results. Several experimentalist have measured the first absorption peak in phenanthrene to be a very weak one, due to a dipole forbidden (D.F.) state^{1,12,35,39}. In particular Klevens *et al.*³⁵, Okomoto *et al.*¹², Clar *et al.*¹ and Salama *et al.*³⁹ measured its locations at 3.50 eV, 3.57 eV, 3.59 eV and 3.61 eV, respectively. Our standard parameter value of the D.F. state at 3.35 eV is closer to the experimental values than the screened parameter value computed to be 2.96 eV. Both our screened and standard parameter calculations

predict this D.F. state to be of 1A_1 symmetry, in agreement with the work of Skancke⁴¹. Our PPP-CI calculations predict that the first dipole allowed state is not the most intense one, in contradiction with the TB results. We would like to point out that this PPP-CI result is in perfect agreement with the experimental measurement of Klevens *et al.*³⁵, Okamoto *et al.*¹² and Clar *et al.*¹. The location of the first dipole allowed peak, which is also the optical gap, was calculated to be 4.31 eV with screened parameters, and 4.26 eV with standard parameters. These values are in good agreement with the experimental values which are measured in the range 4.09–4.36 eV (see Table III). In particular, our results are in excellent agreement with the values 4.24 eV, 4.25 eV, and 4.36 eV, reported by Clar *et al.*¹, Salama *et al.*³⁹, and Halasinski *et al.*⁴⁰, respectively.

As far as higher energy peaks are concerned, our screened parameter spectra has a peak at 4.62 eV which is in excellent agreement with the reported value 4.64 eV by Halasinski *et al.*⁴⁰. The next peak is the most intense (MI) peak in our calculated spectrum for both screened as well as standard parameter calculations, and it is located at 4.93 eV and 5.19 eV, respectively. Clar *et al.*¹ experimentally measured the most intense peak at 4.93 eV which exactly matches with our screened parameter value. The reported value of MI peak by Klevens *et al.*³⁵ (4.88 eV) and Salama *et al.*³⁹ (4.80 eV) are also very close with our obtained screened parameter value, while the MI peak obtained using standard parameter is little bit on the higher side compared to the experimental results.

After that Halasinski *et al.*⁴⁰ report a peak at 5.78 eV, while Clar *et al.*¹ report one at 5.65 eV. Our screened parameter peak at 5.71 eV is in excellent agreement with Halasinski *et al.*⁴⁰, while the standard parameter peak at 5.59 eV, is in very good agreement with the peak reported by Clar *et al.*¹.

Next experimental peak located at 6.62 eV, reported by Klevens *et al.*³⁵, is in good agreement with our screened parameter peak computed at 6.74 eV. The highest measured peak located at 6.99 eV, reported by Klevens *et al.*³⁵ is in excellent agreement with the peaks obtained both from screened and standard parameter calculations at 7.05 eV and 6.96 eV, respectively. Furthermore, we have computed several higher energy peaks as well, for which no experimental results exist. We hope that in future measurements of the absorption spectrum of phenanthrene, energy range beyond 7 eV will be explored.

Dutta and Mazumdar^{48,49} studied the ground state of metal-intercalated crystalline phenanthrene using both *ab initio* density functional theory (DFT), and PPP model based

approaches, with the aim of understanding the nature of superconductivity in these materials. Parac *et al.*³⁶ have computed the absorption spectra of phenanthrene using time-dependent DFT (TDDFT) and time-dependent PPP (TDPPP) method, while Mallocci *et al.*³⁷ have computed the same using DFT and TDDFT method. By using PPP model at the singles-CI level, Skancke *et al.* and Hedges *et al.* have also computed the absorption spectra of phenanthrene. We present the results of these authors in Table III, from where it is obvious that their calculated peak locations lie in a broad spectral range. Given the fact that peaks measured by various experiments also lie in a broad spectral range, the agreement between these theoretical results and experiments is quite reasonable. The detailed wave function analysis of all the excited states contributing to peaks in the computed spectra of phenanthrene, is presented in Tables S1-S2 of Supporting Information.

Table III: Comparison of computed peak locations in the spectra of phenanthrene with the experimental, and other theoretical values; all energies are in eV. Columns with headings Scr/Std contain results of calculations performed using the screened/standard parameters in the PPP model. MI denotes the peak of maximum intensity, OG denotes the peak corresponding to the optical gap, and D.F. indicates the dipole forbidden state.

Experimental	Theoretical (other authors)	This Work	
		Scr	Std
3.50 ³⁵ (D.F.), 3.57 ¹² (D.F.), 3.59 ¹ (D.F.), 3.61 ³⁹ (D.F.),	3.65 ^a /3.82 ^b /3.97 ^c (D.F.) ³⁶ , 4.01 ⁴¹ (D.F.), 4.22 ⁴³ (D.F.)	2.96 (¹ A ₁) (D.F.)	3.35 (¹ A ₁) (D.F.)
4.09 ³⁵ (OG), 4.17 ¹² (OG), 4.24 ^{1,38} (OG), 4.25 ³⁹ (OG), 4.36 ⁴⁰ (OG),	3.91 ^a /4.21 ^c /4.34 ^{b36} (OG), 4.19 ^c /4.67 ^{d37,42} (OG), 4.36 ⁴¹ (OG), 4.60 ⁴³ (OG),	4.31 (¹ B ₁) (OG)	4.26 (¹ B ₁) (OG)
4.34 ¹² ,			
4.42 ³⁹ , 4.44 ¹² , 4.53 ⁴⁰ , 4.56 ³⁹ , 4.64 ⁴⁰ (MI),	—	4.62 (¹ A ₁)	—
4.80 ³⁹ (MI) , 4.93 ¹ (MI), 4.88 ³⁵ (MI), 5.10 ⁴⁰ , 5.27 ⁴⁰ ,	—	4.93 (¹ B ₁) (MI)	5.19 (¹ A ₁ / ¹ B ₁) (MI)
5.65 ¹ , 5.78 ⁴⁰ , 5.84 ³⁵ ,	5.45 ⁴³ , 5.47 ⁴² (MI), 5.52 ⁴¹ ,5.89 ⁴¹ (MI),	5.71 (¹ A ₁ / ¹ B ₁)	5.59 (¹ A ₁)
—	6.01 ⁴² , 6.25 ⁴¹ ,	6.07 (¹ B ₁)	6.10 (¹ B ₁)
—	6.38 ⁴² ,	6.49 (¹ A ₁)	6.40 (¹ B ₁)
6.62 ³⁵	6.72 ⁴² , 6.75 ⁴² ,	6.74 (¹ B ₁)	—
6.99 ³⁵	6.90 ⁴¹ , 7.39 ⁴² ,	7.05 (¹ A ₁)	6.96 (¹ A ₁ / ¹ B ₁)
^a TDDFT(BP86) method, ^b TDPPP method, ^c TDDFT(B3LYP) method and ^d DFT(Kohan-Sham) method			

Chrysene

Chrysene has C_{2h} symmetry, and Okamoto *et al.*¹², Klevens *et al.*³⁵, Clar *et al.*¹ and Becker *et al.*⁴⁴ have reported the measurements of its absorption spectrum. In Fig. 3 (a) and (b), we present our calculated spectra using the screened and standard parameters, respectively, within the PPP-CI approach, and in Table IV, we have compared the experimental peak locations with our results, and those of other theoretical calculations. The first peaks observed experimentally by Klevens *et al.*³⁵, Okamoto *et al.*¹², Becker *et al.*⁴⁴ and Clar *et al.*¹ are located at 3.40 eV, 3.42 eV, 3.43 eV, and 3.44 eV respectively, and again correspond to a dipole forbidden (D.F.) state. Using the standard parameters, we obtain the D.F. state at 3.33 eV, which agrees well with the measured values. The screened parameter value computed at 3.11 eV, is slightly lower as compared to the experimental values. Both screened and standard parameter calculation predict the D.F. state to be of 1B_u symmetry, in agreement with the work of Skancke⁴¹.

The intensity of the first dipole allowed peak, corresponding to the optical gap, was not found to be maximum in our calculated spectra. This result is in perfect agreement with the measurements of Klevens *et al.*³⁵, Okamoto *et al.*¹², Becker *et al.*⁴⁴ and Clar *et al.*¹, and in disagreement with the results of the TB model. Our calculations predict this peak at 3.86 eV using screened parameters, and 3.96 eV using standard parameters. As is obvious from Table III, the experimental values of the optical gap range from 3.74 eV to 3.89 eV, implying that both the calculated values of optical gap are quite close to the experimental values. In particular, we also note that the Okamoto *et al.*¹² and Becker *et al.*⁴⁴ reported the values of optical gap at 3.84 eV, and 3.87 eV, respectively, almost in perfect agreement with our screened parameter value 3.86 eV. The standard parameter value of 3.96 eV is slightly higher than the highest measured value 3.89 eV by Mallory *et al.*⁴⁵ and Clar *et al.*¹.

The second peak is the most intense (MI) peak in our calculated spectrum for both the screened and the standard parameters, and is located at 4.52 eV, and 5.08 eV, respectively. Okamoto *et al.*¹² experimentally measured the most intense peak at 4.54 eV which almost exactly matches with our screened parameter value. The reported value of MI peak by Klevens *et al.*³⁵ (4.61 eV), Becker *et al.*⁴⁴ (4.63 eV), and Clar *et al.*¹ (4.64 eV) are slightly higher than the screened parameter value, while the standard parameter result is significantly higher than the experimental values.

As far as higher energy peaks are concerned, Klevens *et al.*³⁵, and Becker *et al.*⁴⁴ found a peak at 5.13 eV, and, Clar *et al.*¹ found one at 5.14 eV. In our computed spectra, we have a peak at 5.09 eV using screened parameters, and 5.08 eV using standard parameters, both of which are in good agreement with experiments. After that, in our standard parameter spectrum we have a peak at 5.76 eV, which is in very good agreement with the 5.71 eV peak detected by Becker *et al.*⁴⁴, while the screened parameter peak at 5.81 eV is somewhat higher as compared to the experiments. Next experimental peak located at 6.36 eV, reported by Klevens *et al.*³⁵, is in perfect agreement with our standard parameter peak computed at 6.38 eV. We have a screened parameter peak at 6.52 eV which is in reasonable agreement with a peak at 6.43 eV, measured by Becker *et al.*⁴⁴. The highest measured peak located at 6.73 eV reported by Klevens *et al.*³⁵ is at a slightly lower energy as compared to the corresponding screened parameter peak at 6.86 eV. Furthermore, we have computed several higher energy peaks as well, for which no experimental results exist. We hope that in future measurements of the absorption spectrum of chrysene, in higher energy range will be probed.

First principles TDDFT method was employed to calculate the absorption spectrum by Parac *et al.*³⁶ and Mallocci *et al.*³⁷. Mallocci *et al.*³⁷ also computed the absorption spectrum using the first principles DFT. Additionally, PPP model based calculations were performed by Parac *et al.*³⁶, Skancke *et al.*⁴¹, Ham *et al.*⁴⁶ and Hedges *et al.*⁴³.

The predictions on the location of D.F. state by other authors are in a broad energy range 3.48-4.13 eV^{36,41,43,46}, while the experimental values are in a very narrow range 3.40-3.44 eV^{1,12,35,44}. This means that most of the calculations of other authors overestimate the experimental results. Regarding the optical gap, calculations of other authors predict it in the range 3.40-4.22 eV, while the experimental values are in the range 3.74-3.89 eV, implying that most other calculations either underestimate or overestimate the experimental values. But we note that the optical gaps computed using the TDDFT approach with B3LYP functional by Parac *et al.*³⁶, and Mallocci *et al.*³⁷, are in good agreement with experiments. As far as the location of MI peak is concerned, results of other authors are either below, or significantly above the experimental value. The wave function of the excited states contributing to peaks in the computed spectra of chrysene, are presented in Tables S3-S4 of Supporting Information.

Table IV: Comparison of computed peak locations in the spectra of chrysene with the experimental values, and other theoretical values; all energies are in eV. Rest of the information is same as in the caption of Table III.

Experimental	Theoretical (other authors)	This Work	
		Scr	Std
3.40 ³⁵ (D.F.), 3.42 ¹² (D.F.), 3.43 ⁴⁴ (D.F.), 3.44 ¹ (D.F.)	3.48 ^a /3.62 ^b /3.75 ^{c36} (D.F.), 3.47 ⁴⁶ (D.F.), 4.10 ⁴³ (D.F.) 4.13 ⁴¹ (D.F.),	3.11 (¹ B _u) (D.F.)	3.33 (¹ B _u) (D.F.)
3.74 ³⁵ (OG), 3.84 ¹² (OG), 3.87 ⁴⁴ (OG), 3.89 ^{1,45} (OG),	3.40 ^a /3.92 ^b /3.82 ^{c36} (OG), 3.73 ^c /4.21 ^{d37,42} (OG) 3.90 ⁴⁶ (OG), 4.13 ⁴¹ (OG), 4.22 ⁴³ (OG)	3.86 (¹ B _u) (OG)	3.96 (¹ B _u) (OG)
4.00 ¹² , 4.17 ¹²	—	—	—
4.54 ¹² (MI), 4.61 ³⁵ (MI), 4.63 ⁴⁴ (MI), 4.64 ¹ (MI), 4.71 ¹²	4.26 ^{41,42}	4.52 (¹ B _u) (MI)	—
5.13 ^{35,44} , 5.14 ¹ ,	4.84 ⁴² (MI), 4.93 ⁴⁶ , 5.35 ⁴⁶ , 5.39 ⁴³ , 5.47 ⁴³	5.09 (¹ B _u)	5.08 (¹ B _u) (MI)
5.59 ⁴⁴ , 5.65 ³⁵ , 5.71 ⁴⁴	5.43 ⁴² , 5.48 ⁴¹ , 5.75 ⁴¹ (MI),	5.81 (¹ B _u)	5.76 (¹ B _u)
—	6.13 ⁴²	6.00 (¹ B _u)	—
6.36 ³⁵ , 6.43 ⁴⁴	6.36 ⁴¹	6.52 (¹ B _u)	6.38 (¹ B _u)
6.73 ³⁵	6.99 ⁴²	6.86 (¹ B _u)	7.17 (¹ B _u)
—	7.32 ⁴¹ ,	7.32 (¹ B _u)	7.37 (¹ B _u)
^a TDDFT(BP86) method, ^b TDPPP method, ^c TDDFT(B3LYP) method and ^d DFT(Kohan-Sham) method			

Picene has C_{2v} symmetry, and Okamoto *et al.*¹², Clar *et al.*¹ and Fanetti *et al.*⁴⁷ have reported the measurements of its absorption spectrum. In Fig. 3 (a) and (b), we present our calculated spectra using the screened and standard parameters, respectively, within the PPP-CI approach, and in Table V, we have compared the locations of various peaks obtained in our calculations with the experimental results, and other theoretical results. The first peak corresponding to the dipole forbidden (D.F.) state was measured to be at 3.30 eV by Okamoto *et al.*,¹² and Clar *et al.*¹, while Fanetti *et al.*⁴⁷ measured it at 3.31 eV. Our standard parameter calculation predicts the D.F. state at 3.33 eV, in excellent agreement with the experiments, while the screened parameter value at 3.20 eV is slightly lower than the experiments. Both sets of calculations predict the D.F. state to be of 1A_1 symmetry.

The first dipole allowed state is computed to be of 1B_1 symmetry, and leads to fairly intense absorption peaks located at 3.75 eV in the screened parameter spectrum, and 3.88 eV in the standard parameter spectrum. As it is obvious from Table III, the experimental values of the optical gap range from 3.76 eV to 3.82 eV. Thus, we find that both our screened and standard parameter of optical gap are quite close to the range of experimental values. We also note that the Okamoto *et al.*¹² and Mallory *et al.*⁴⁵ reported the value of optical gap at 3.76 eV, and the Clar *et al.*¹ reported it at 3.77 eV, in excellent agreement with our screened parameter value. While our standard parameter value 3.88 eV agrees well with the optical gap value 3.82 eV, measured by Fanetti *et al.*⁴⁷. Furthermore, our calculation predict that this peak is not the most intense one, in disagreement with the TB model results, and in complete agreement with the experiments^{1,12,47}.

As far as higher energy peaks are concerned, our screened parameter spectrum has a peak at 4.54 eV which is in very good agreement with a peak at 4.57 eV measured by Fanetti *et al.*⁴⁷. The next peaks which are the most intense (MI) ones in our calculated spectra using both screened and standard parameters, are located at 4.87 eV and 4.79 eV, respectively. Okamoto *et al.*¹² measured a peak at 4.75 eV, which is in very good agreement with the location of our standard parameter peak. A peak measured at 4.85 eV by Fanetti *et al.*⁴⁷ is in excellent agreement with the energy of our screened parameter peak.

Our calculated peaks at 5.22 eV (screened) and 5.24 eV (standard) are the nearest peaks to the highest measured peak at 5.08 eV reported¹ by Fanetti *et al.*⁴⁷. Additionally, we have

computed several higher energy peaks as well, for which no experimental results exist. We hope that in future measurements of the absorption spectrum of picene, energy range beyond 5 eV will be explored.

The measured experimental value of D.F. state are in very tight energy range 3.30-3.31 eV^{1,12,45,47}, while the D.F. state calculated by other authors lie in a broad spectral range 3.18-4.33 eV^{36,37,43}. As far as optical gap is concerned, the computed values of other authors are in the range of 3.32-4.13 eV, while the experimental values are in the range 3.76-3.82 eV. Therefore, both for D.F. state and optical gap several other calculations have either underestimated or overestimated the data. But we note that Parac and Grimme³⁶ have obtained the optical gap value at 3.72 eV using TDDFT method which is in good agreement with experimental value 3.76 eV. They have also calculated the optical gap value using TDPPP method, which is also in good agreement with the experimental results. The detailed analysis of wave functions of the excited states contributing to peaks in the calculated spectra of picene, is presented in Tables S5-S6 of Supporting Information.

Table V: Comparison of computed peak locations in the spectra of picene with the experimental values, and other theoretical values; all energies are in eV. Rest of the information is same as in the caption of Table III.

Experimental	Theoretical (other authors)	This Work	
		Scr	Std
3.30 ^{1,12} (D.F.), 3.31 ⁴⁷ (D.F.)	3.18 ^a /3.49 ^b /3.56 ^{c36} (D.F.), 4.33 ⁴³ (D.F.)	3.20 (¹ A ₁)(D.F.)	3.33 (¹ A ₁)(D.F.)
3.76 ^{12,45} (OG), 3.77 ¹ (OG), 3.82 ⁴⁷ (OG),	3.32 ^a /3.83 ^b /3.72 ^{c36} (OG), 3.70 ^c /4.19 ^{d37} (OG), 4.13 ⁴³ (OG),	3.75 (¹ B ₁)(OG)	3.88 (¹ B ₁)(OG)
3.93 ¹² , 3.98 ⁴⁷ , 4.06 ¹² , 4.13 ⁴⁷ ,	—	—	—
4.26(MI) ¹² , 4.32 ¹ (MI), 4.39 ⁴⁷ (MI), 4.45 ¹² , 4.57 ⁴⁷ ,	—	4.54 (¹ A ₁)	—
4.72 ⁴⁷ , 4.75 ¹² , 4.85 ⁴⁷ ,	—	4.87(MI) (¹ A ₁ / ¹ B ₁)	4.79(MI) (¹ A ₁ / ¹ B ₁)
5.08 ⁴⁷	5.13 ⁴³ , 5.22 ⁴³	5.22 (¹ B ₁)	5.24 (¹ A ₁)
^a TDDFT(BP86) method, ^b TDPPP method, ^c TDDFT(B3LYP) method and ^d DFT(Kohan-Sham) method			

Fulminene

Fulminene has C_{2h} symmetry, and Okamoto *et al.*^{5,12} and Mallory *et al.*⁴⁵ have measured the absorption in fulminene. In Fig. 3 (a) and (b), we present our calculated spectra using the screened and standard parameters, respectively, within the PPP-CI approach, and in Table VI, we have compared the experimental results, and theoretical results of other authors, with our calculations. The detailed wave functions analysis of all the excited states contributing to peaks in the computed spectra of fulminene, is presented in Tables S7-S8 of Supporting Information.

The first peak observed experimentally by Okamoto *et al.*¹² is located at 3.24 eV, and it corresponds to a dipole forbidden (D.F.) state. Both our standard parameter and screened parameter calculations predict the symmetry of this state to be 1B_u , and located at 3.07 eV, and 2.86 eV, respectively. This implies that our calculated locations of the D.F. state are lower than the experimental value, with the screened parameter value being significantly lower.

The first dipole allowed peak, corresponding to the optical gap, was measured to be at 3.14 eV for the thin film sample by Okamoto *et al.*⁵, and 3.65 eV, and 3.66 eV for the solution sample, by Okamoto *et al.*⁵, and Mallory *et al.*⁴⁵, respectively. Our screened parameter calculations predict the optical gap to be 3.34 eV, which is closer to the measured value of thin film sample, while our standard parameter value at 3.52 eV is closer to the solution based sample. This is understandable on physical grounds because, in thin films, electron correlations may be getting screened due to presence of other molecules, an effect screened parameters may be mimicking. We also note that intensity of the first dipole allowed peak is not maximum when compared to other peaks, in agreement with the measurements of the Okamoto *et al.*⁵.

As far as higher energy features are concerned, our screened parameter spectrum has a peak at 4.01 eV, which is in good agreement with the peaks measured at 3.95 eV¹², and 4.08 eV⁵, in solution, and thin film, based samples, respectively. The next peak is the most intense (MI) one in our calculated spectrum for the both screened and standard parameters, located at 4.37 eV, and 4.54 eV, respectively. In solution based spectrum the most intense peak lies at 4.17 eV¹² which is closer to the screened parameter value, than the standard one. Furthermore, we have computed several higher energy peaks as well, for which no experimental results exist. We hope that in future measurements of the absorption spectrum of fulminene, the energy range beyond 5 eV will be explored.

The only other calculation on fulminene is by Mallocci *et al.*³⁷, who reported the values of optical gap at 3.47 eV (TDDFT approach), and 4.00 eV (Kohn-Sham). The former value is within the range of experimental measurements, while the latter is well above it.

Table VI: Comparison of computed peak locations in the spectra of fulminene with the experimental values, and other theoretical values; all energies are in eV. Rest of the information is same as in the caption of Table III.

Experimental	Theoretical (other authors)	This Work	
		Scr	Std
3.24 ¹² (D.F.)	—	2.86 (¹ B _u)(D.F.)	3.07 (¹ B _u)(D.F.)
3.14 ⁵ (OG), 3.65 ¹² (OG), 3.66 ⁴⁵ (OG),	3.47 ^c / 4.00 ^{d37} (OG)	3.34 (¹ B _u)(OG)	3.52 (¹ B _u)(OG)
3.29 ⁵ , 3.44 ⁵ ,			
3.90 ⁵ , 3.80 ¹² , 3.95 ¹² , 4.08 ⁵	—	4.01 (¹ B _u)	—
4.17 ¹² (MI), 4.36 ¹² , 4.66 ¹²	—	4.37 (¹ B _u)(MI)	4.54 (¹ B _u)(MI)
^c TDDFT(B3LYP) method and ^d DFT(Kohan-Sham) method			

[7]Phenacene

[7]phenacene has C_{2v} symmetry, and Okamoto *et al.*⁵, and Mallory *et al.*⁴⁵ have reported the measurements of its absorption spectrum. In Fig. 3 (a) and (b), we present our calculated spectra using the screened and standard parameters, respectively, within the PPP-CI approach, and in Table VII, we have compared the experimental results, and theoretical results of other authors, with our calculations. Analysis of the calculated CI wave functions of the excited states contributing to the absorption spectra, is presented in Tables S9-S10 of Supporting Information.

Our calculations predict the dipole forbidden state to be of ¹A₁ symmetry, located at 2.96 eV(screened parameters) and 3.31 eV (standard parameters). Because no prior experimental measurements of D.F. state are available for [7]phenacene, our results could be tested in future experiments.

On comparing the relative intensity of first dipole allowed peak, corresponding to the optical gap, we find that it is not of maximum intensity, in agreement with the measurements^{5,45}. Our calculations predicts this peak at 3.34 eV (screened parameters), and at 3.68 eV (stan-

standard parameters). We note that the Okamoto *et al.*⁵ reported the value of optical gap at 3.10 eV, which is closer to our screened parameter value, while our standard parameter value is in very good agreement with 3.60 eV, measured by Mallory *et al.*⁴⁵.

As far as higher energy peaks are concerned, our screened parameter spectra has a peak at 3.88 eV which is in excellent agreement with the measured values 3.87 eV⁴⁵, and 3.90 eV⁵. The next peak is the most intense (MI) peak in our calculated spectrum located at 4.20 eV (screened parameters) and 4.68 eV (standard parameters). Okamoto *et al.*⁵ and Mallory *et al.*⁴⁵ experimentally measured the most intense peak at 4.08 eV which is a little lower than our screened parameter value. Furthermore, we have computed several higher energy peaks as well, for which no experimental results exist. We hope that in future measurements of the absorption spectrum of [7]phenacene, the energy range beyond 5 eV will be probed.

The only other calculation on [7]phenacene is by Mallocci *et al.*³⁷, who reported the values of optical gap at 3.50 eV (TDDFT approach), and 4.00 eV (Kohn-Sham). The former value is within the range of experimental measurements, while the latter is well above it.

Table VII: Comparison of computed peak locations in the spectra of [7]phenacene with the experimental values, and other theoretical values; all energies are in eV. Rest of the information is same as in the caption of Table III.

Experimental	Theoretical (other authors)	This Work	
		Scr	Std
—	—	2.96 (¹ A ₁)(D.F.)	3.31 (¹ A ₁)(D.F.)
3.10 ⁵ (OG), 3.29 ⁵ , 3.44 ⁵ , 3.60 ⁴⁵ (OG),	3.50 ^c /4.00 ^{d,37} (OG),	3.34 (¹ B ₁) (OG)	3.68 (¹ B ₁) (OG)
3.87 ⁴⁵ , 3.90 ⁵	—	3.88 (¹ A ₁)	—
4.08 ^{5,45} (MI)	—	4.20 (¹ A ₁ / ¹ B ₁) (MI)	4.68 (¹ B ₁) (MI)
^c TDDFT(B3LYP) method; ^d DFT(Kohn-Sham) method			

[8]Phenacene

[8]phenacene has C_{2h} symmetry, and Okamoto *et al.*⁵ have reported the measurement its

absorption spectrum. In Fig. 3 (a) and (b), we present our calculated spectra using the screened and standard parameters, respectively, within the PPP-CI approach, and in Table VIII, we have compared the experimental results, with our calculations. In this molecule we have calculated a dipole forbidden (D.F.) state of 1B_u symmetry, located at 2.84 eV with screened parameters, and 3.13 eV with standard parameters. However, we are unable to compare our results with the experiments, because no measurements of this state have been performed so far.

In our calculated spectra, the first dipole allowed peak corresponding to the optical gap is not the most intense peak of the spectrum, in full agreement with the experimental measurements⁵. The calculated locations of this peak is 3.11 eV using screened parameters, and 3.41 eV using standard parameters. We find that our screened parameter results are in excellent agreement with the experimentally measured value of 3.08 eV⁵.

As far as higher energy peaks are concerned, our screened parameter spectrum has a peak at 3.87 eV which is a bit higher than the measured peak at 3.64 eV⁵. The next peak is the most intense (MI) peak in our calculated spectrum for the both screened as well as standard parameters, and is located at 4.08 eV, and 4.48 eV, respectively. Okamoto *et al.*⁵ experimentally measured the most intense peak at 4.00 eV which is in very good agreement with our screened parameter value. Furthermore, we have computed several higher energy peaks as well, for which no experimental results exist. We hope that in future measurements of the absorption spectrum of [8]phenacene, energy range beyond 4 eV will be explored. Detailed information about the wave functions of the excited states contributing to peaks in the computed spectra, can be obtained in Tables S11-S12 of Supporting Information.

Table VIII: Comparison of computed peak locations in the spectra of [8]phenacene with the experimental values; all energies are in eV. Rest of the information is same as in the caption of Table III.

Experimental	This Work	
	Scr	Std
—	2.84 (1B_u)(D.F.)	3.13 (1B_u)(D.F.)
3.08 ⁵ (OG), 3.26 ⁵ , 3.44 ⁵	3.11(1B_u)(OG)	3.41 (1B_u)(OG)
3.64 ⁵	3.87 (1B_u)	—
4.00 ⁵ (MI)	4.08 (1B_u)(MI)	4.48 (1B_u)(MI)

[9]Phenacene

[9]phenacene has C_{2v} symmetry, and Shimo *et al.*¹¹ have reported the measurement of its absorption spectrum. In Fig. 3 (a) and (b), we present our calculated spectra using the screened and standard parameters, respectively, within the PPP-CI approach, and in Table IX, we have compared the experimental results, with our calculations. Additionally, detailed information about the excited states contributing to peaks in the computed spectra is presented in Tables S13-S14 of Supporting Information.

Our calculations locate a dipole forbidden (D.F.) state of 1A_1 symmetry, at 2.92 eV, with screened parameters, and at 3.29 eV with standard parameters. However, we are unable to compare our results with the experiments, because no measurements of this state have been performed so far.

In this molecule as well, our calculations predict that the first dipole-allowed peak corresponding to the optical gap, is not the most intense peak of the spectrum, in full agreement with the experiment,¹¹ and in disagreement with the results of the TB model calculations. As far as the value of optical gap is concerned, our calculations predict it to be 3.09 eV obtained using the screened parameters, and 3.46 eV using the standard parameters. We note that our screened parameter value is in very good agreement with the value 3.05 measured by Shimo *et al.*¹¹.

As far as higher energy peaks are concerned, our screened parameter spectrum has a peak

at 3.54 eV, which is somewhat higher than 3.33 eV measured by Shimo *et al.*¹¹. The most intense (MI) peaks in our calculated spectra for screened as well as standard parameters are located at 3.98 eV, and 5.0 eV, respectively. In the experimental spectrum of Shimo *et al.*¹¹, the intensity appears to increase monotonically in the region 3.60-4.00 eV, beyond which no measurements exist. This implies that the maximum intensity peak is at an energy higher than 4.00 eV, which we hope will be confirmed in future measurements. Furthermore, we have computed several higher energy peaks as well, which we hope will also be verified in future measurements beyond 4 eV. We are unable to compare our results with calculations of other authors, because our calculations appear to be the first ones on this molecule.

Table IX: Comparison of computed peak locations in the spectra of [9]phenacene with the experimental values; all energies are in eV. Rest of the information is same as in the caption of Table III.

Experimental	This Work	
	Scr	Std
—	2.92 (¹ A ₁)(D.F.)	3.29 (¹ A ₁)(D.F.)
3.05 ¹¹ (OG), 3.22 ¹¹	3.09 (¹ B ₁)(OG)	3.46 (¹ B ₁)(OG)
3.33 ¹¹	3.54 (¹ A ₁)	—
—	3.98(¹ A ₁ / ¹ B ₁) (MI)	—
—	4.38 (¹ A ₁)	4.21 (¹ A ₁ / ¹ B ₁)
—	4.8 (¹ A ₁ / ¹ B ₁)	—
—	5.13 (¹ A ₁ / ¹ B ₁)	5.0 (¹ A ₁)(MI)

C. Comparison between Phenacenes and Polyacenes

As mentioned in the Introduction section, phenacenes and polyacenes are isomers, *i.e.* they have same chemical formula but different structural arrangement. In polyacenes, benzene rings are fused in a straight line and they belong to D_{2h} point group. While, in phenacenes, benzene rings are fused in a zig-zag manner, leading either to C_{2v} or C_{2h} symmetry. In an earlier work in our group, Sony *et al.*¹⁷ computed the absorption spectra

of oligoacenes ranging from naphthalene to heptacene, and, later on Chakraborty *et al.*²⁴ extended the work till decacene. In Table X we compare our calculated optical gaps for isomers containing 3 to 9 benzene rings, and we find that irrespective of parameters used, the optical gaps of $[n]$ phenacenes are always larger than those of acene- n . We also note the relative difference in the optical gaps of two set of compounds increases with the increasing conjugation length. These facts are also verified in the optical absorption experiments on phenacenes cited in the present work, as well those on acenes reviewed in our earlier work.¹⁷ Additionally, Roth *et al.*⁵⁰ performed a comparative study of singlet states in two of the smallest phenacenes (phenanthrene and chrysene), and acenes (anthracene and tetracene) in the crystalline phase, using the electron-energy-loss spectroscopy (EELS), and concluded that absorptions occur in acenes at much lower energies as compared to corresponding phenacenes. This, combined with our theoretical calculations, suggests that the lowest singlet excitations in both acene and phenacene molecular crystals are intramolecular in nature. Thus, experimental and theoretical evidence suggests that as far as optoelectronic device applications are concerned, phenacenes will be useful in higher frequency range, as compared to oligoacenes.

Table X: Comparison of the optical gaps of phenacenes and oligoacenes, computed using the PPP-CI approach.

Phenacenes (This work)	Optical gap (eV)		Oligoacenes (Sony <i>et al.</i> ¹⁷ and Chakraborty <i>et al.</i> ²⁴)	Optical gap (eV)	
	Scr.	Std.		Scr.	Std.
Phenanthrene	4.31	4.26	Anthracene ¹⁷	3.55	3.66
Chrysene	3.86	3.96	Tetracene ¹⁷	2.97	3.16
Picene	3.75	3.88	Pentacene ¹⁷	2.65	2.86
Fulminene	3.34	3.52	Hexacene ¹⁷	2.38	2.71
[7]Phenacene	3.34	3.68	Heptacene ¹⁷	2.24	2.63
[8]Phenacene	3.11	3.41	Octacene ²⁴	1.49	2.24
[9]Phenacene	3.09	3.46	Nonacene ²⁴	1.46	1.82

V. SUMMARY AND CONCLUSIONS

In this paper, we presented the results of our calculations of optical absorption spectra of $[n]$ phenacenes, with $n = 3-9$. The calculations were performed using both the tight-binding, and PPP models, and for the case of PPP model, electron correlation effects were taken into account within the configuration-interaction approach. Our calculations reveal that the inclusion of electron correlation effect is very important for the correct qualitative and quantitative description of optical properties of these materials. For example, optical gaps predicted by TB model are much smaller than their experimental values, and the predictions of our PPP-CI calculations. We find our PPP-CI values of the optical gaps are generally in very good agreement with the experimental values. Furthermore, the TB model predicts for all the molecules that the first dipole allowed peak corresponding the optical gap is the most intense peak of the spectrum, in complete disagreement with the experiments, as well as results of our PPP-CI calculations. Moreover, predictions of our PPP-CI calculations on absorption peaks higher than the optical gap are also in very good agreement with the experiments.

We also compared the calculated optical gaps of $[n]$ phenacene with their isomeric oligoacenes, and noted that gaps of $[n]$ phenacenes are significantly larger. This is in agreement not only with numerous optical absorption experiments performed on these molecules, but also with a comparative EELS study of crystalline phenanthrene, chrysenes, anthracene, and tetracene.⁵⁰ This further validates our theory, and also confirms that the lowest optical excitations in these materials are intramolecular excitons. Furthermore, this suggests that $[n]$ phenacenes can have optoelectronic applications in the higher energy range.

In this paper, we have confined ourselves to the study of the optical properties of $[n]$ phenacenes for their ground states, i.e., in the singlet manifold. However, in these materials, triplet states, and their optics, are also very interesting, from the point of view of light harvesting through the route of singlet fission, which we aim to study in future. We also plan to explore the non-linear optical processes in phenacenes such as two-photon absorption, and third-harmonic generation, in future works.

ACKNOWLEDGMENTS

This research was supported in part by Department of Science and Technology, Government of India, under project no. SB/S2/CMP-066/2013.

* dkriitb@gmail.com

† shukla@phy.iitb.ac.in

- ¹ E. Clar and R. Schoental, *Polycyclic hydrocarbons*, Vol. 1 (Springer, 1964).
- ² E. Dwek, R. Arendt, D. Fixsen, T. Sodroski, N. Odegard, J. Weiland, W. Reach, M. Hauser, T. Kelsall, S. Moseley, *et al.*, *The Astrophysical Journal* **475**, 565 (1997).
- ³ C.-E. Boström, P. Gerde, A. Hanberg, B. Jernström, C. Johansson, T. Kyrklund, A. Rannug, M. Törnqvist, K. Victorin, and R. Westerholm, *Environmental health perspectives* **110**, 451 (2002).
- ⁴ A. T. Lawal, *Cogent Environmental Science* **3**, 1339841 (2017), <https://www.tandfonline.com/doi/pdf/10.1080/23311843.2017.1339841>.
- ⁵ H. Okamoto, R. Eguchi, S. Hamao, H. Goto, K. Gotoh, Y. Sakai, M. Izumi, Y. Takaguchi, S. Gohda, and Y. Kubozono, *Scientific reports* **4**, 5330 (2014).
- ⁶ G. Witte and C. Wöll, *Journal of Materials Research* **19**, 1889 (2004).
- ⁷ F. Cicoira and C. Santato, *Advanced Functional Materials* **17**, 3421 (2007).
- ⁸ P. Raghunath, M. A. Reddy, C. Gouri, K. Bhanuprakash, and V. J. Rao, *The Journal of Physical Chemistry A* **110**, 1152 (2006).
- ⁹ Y. Yamashita, *Science and Technology of Advanced Materials* **10**, 024313 (2009), <https://doi.org/10.1088/1468-6996/10/2/024313>.
- ¹⁰ Y. Kubozono, X. He, S. Hamao, K. Teranishi, H. Goto, R. Eguchi, T. Kambe, S. Gohda, and Y. Nishihara, *European Journal of Inorganic Chemistry* **2014**, 3806 (2014).
- ¹¹ Y. Shimo, T. Mikami, S. Hamao, H. Goto, H. Okamoto, R. Eguchi, S. Gohda, Y. Hayashi, and Y. Kubozono, *Scientific reports* **6**, 21008 (2016).
- ¹² H. Okamoto, M. Yamaji, S. Gohda, K. Sato, H. Sugino, and K. Satake, *Research on Chemical Intermediates* **39**, 147 (2013).
- ¹³ N. Komura, H. Goto, X. He, H. Mitamura, R. Eguchi, Y. Kaji, H. Okamoto, Y. Sugawara,

- S. Gohda, K. Sato, *et al.*, Applied Physics Letters **101**, 083301 (2012).
- ¹⁴ Y. Shimo, T. Mikami, S. Hamao, H. Goto, H. Okamoto, R. Eguchi, S. Gohda, Y. Hayashi, and Y. Kubozono, Scientific Reports **6**, 21008 (2016), <https://doi.org/10.1038/srep21008>.
- ¹⁵ R. Mitsuhashi, Y. Suzuki, Y. Yamanari, H. Mitamura, N. I. Takashi Kambe, H. Okamoto, A. Fujiwara, M. Yamaji, N. Kawasaki, Y. Maniwa, and Y. Kubozono, Nature **464**, 76 (2010), <https://www.nature.com/articles/nature08859>.
- ¹⁶ K. Gundra and A. Shukla, “A pariser–parr–pople model hamiltonian-based approach to the electronic structure and optical properties of graphene nanostructures,” in *Topological Modelling of Nanostructures and Extended Systems*, edited by A. R. Ashrafi, F. Cataldo, A. Iranmanesh, and O. Ori (Springer Netherlands, Dordrecht, 2013) pp. 199–227.
- ¹⁷ P. Sony and A. Shukla, Phys. Rev. B **75**, 155208 (2007).
- ¹⁸ J. A. Pople, Trans. Faraday Soc. **49**, 1375 (1953).
- ¹⁹ R. Pariser and R. G. Parr, J. Chem. Phys. **21**, 767 (1953).
- ²⁰ A. Shukla, Phys. Rev. B **65**, 125204 (2002).
- ²¹ A. Shukla, Phys. Rev. B **69**, 165218 (2004).
- ²² P. Sony and A. Shukla, Phys. Rev. B **71**, 165204 (2005).
- ²³ P. Sony and A. Shukla, The Journal of Chemical Physics **131**, 014302 (2009).
- ²⁴ H. Chakraborty and A. Shukla, The Journal of Physical Chemistry A **117**, 14220 (2013).
- ²⁵ H. Chakraborty and A. Shukla, The Journal of Chemical Physics **141**, 164301 (2014).
- ²⁶ K. Aryanpour, A. Roberts, A. Sandhu, R. Rathore, A. Shukla, and S. Mazumdar, The Journal of Physical Chemistry C **118**, 3331 (2014).
- ²⁷ K. Aryanpour, A. Shukla, and S. Mazumdar, The Journal of Chemical Physics **140**, 104301 (2014).
- ²⁸ T. Basak, H. Chakraborty, and A. Shukla, Phys. Rev. B **92**, 205404 (2015).
- ²⁹ T. Basak and A. Shukla, Phys. Rev. B **93**, 235432 (2016).
- ³⁰ K. Ohno, Theoretica chimica acta **2**, 219 (1964).
- ³¹ M. Chandross and S. Mazumdar, Phys. Rev. B **55**, 1497 (1997).
- ³² P. Sony and A. Shukla, Computer Physics Communications **181**, 821 (2010).
- ³³ R. Buenker and S. Peyerimhoff, Theor. Chim. Acta **35**, 33 (1974).
- ³⁴ R. J. Buenker, S. D. Peyerimhoff, and W. Butscher, Molecular Physics **35**, 771 (1978).
- ³⁵ H. Klevens and J. Platt, The Journal of Chemical Physics **17**, 470 (1949).

- ³⁶ M. Parac and S. Grimme, *Chemical physics* **292**, 11 (2003).
- ³⁷ G. Mallocci, G. Cappellini, G. Mulas, and A. Mattoni, *Chemical Physics* **384**, 19 (2011).
- ³⁸ J. B. Birks, *Photophysics of aromatic molecules* (1970).
- ³⁹ F. Salama and L. J. Allamandola, *Journal of the Chemical electronic absorption spectra of PAHs Society, Faraday Transactions* **89**, 2277 (1993).
- ⁴⁰ T. Halasinski, F. Salama, and L. Allamandola, *The Astrophysical Journal* **628**, 555 (2005).
- ⁴¹ P. Skancke, *ACTA CHEMICA SCANDINAVICA* **19**, 401 (1965).
- ⁴² G. Mallocci, G. Mulas, and C. Joblin, *Astronomy & Astrophysics* **426**, 105 (2004).
- ⁴³ R. Hedges and L. Phillips, *Theoretical Chemistry Accounts: Theory, Computation, and Modeling (Theoretica Chimica Acta)* **10**, 73 (1968).
- ⁴⁴ R. S. Becker, I. S. Singh, and E. A. Jackson, *The Journal of Chemical Physics* **38**, 2144 (1963).
- ⁴⁵ F. B. Mallory, K. E. Butler, A. C. Evans, E. J. Brondyke, C. W. Mallory, C. Yang, and A. Ellenstein, *Journal of the American Chemical Society* **119**, 2119 (1997).
- ⁴⁶ N. S. Ham and K. Ruedenberg, *The Journal of Chemical Physics* **25**, 13 (1956).
- ⁴⁷ S. Fanetti, M. Citroni, R. Bini, L. Malavasi, G. A. Artioli, and P. Postorino, *The Journal of chemical physics* **137**, 224506 (2012).
- ⁴⁸ T. Dutta and S. Mazumdar, *Phys. Rev. B* **89**, 245129 (2014).
- ⁴⁹ T. Dutta and S. Mazumdar, *arXiv:1607.03198* (2016).
- ⁵⁰ F. Roth, B. Mahns, S. Hampel, M. Nohr, H. Berger, B. Büchner, and M. Knupfer, *The European Physical Journal B* **86**, 66 (2013).

Supporting Information for A Pariser-Parr-Pople Model Based Study of Optoelectronic Properties of Phenacenes

Deepak Kumar Rai* and Alok Shukla†

Department of Physics, Indian Institute of Technology Bombay, Powai, Mumbai 400076, India

arXiv:1810.03482v2 [cond-mat.mtrl-sci] 16 Oct 2018

The following tables contain the excitation energies, dominant many-body wave functions, and transition dipole matrix elements of excited states with respect to the ground state 1^1A_g for C_{2h} , and 1^1A_1 for C_{2v} molecules. The symbols H and L represent the highest occupied molecular orbital (HOMO), and the lowest unoccupied molecular orbital (LUMO), respectively. Many-electron wave functions of various excited states are written as linear combinations of configurations, and the magnitudes of their coefficients are included in parentheses next to them. The configurations are expressed as single-, double-,..., excitations with respect to the closed-shell restricted-Hartree-Fock (RHF) reference state, and the configurations are denoted using arrows from the occupied to unoccupied (virtual) orbitals, representing a given n -particle excitation. The charge conjugate of a given configuration is abbreviated as 'c.c.', while the sign (+/-) preceding 'c.c.' indicates that the two coefficients have (same/opposite) signs. The symbol D.F. denotes a dipole-forbidden state.

Table S1. Excited states giving rise to peaks in the singlet linear absorption spectrum of phenanthrene, computed employing the FCI approach along with the screened parameters in the PPP model Hamiltonian.

Peak	State	E (eV)	Transition Dipole (\AA)	Dominant Contributing Configurations
D.F.	2^1A_1	2.96	0	$ H \rightarrow L + 1\rangle + c.c.$ (0.5564) $ H - 4 \rightarrow L\rangle - c.c.$ (0.1076)
I_x	1^1B_1	4.31	1.2393	$ H \rightarrow L\rangle$ (0.8858) $ H \rightarrow L; H - 3 \rightarrow L + 3; H - 1 \rightarrow L + 1\rangle$ (0.0974)
II_y	4^1A_1	4.62	0.9969	$ H \rightarrow L + 1\rangle - c.c.$ (0.6113) $ H - 1 \rightarrow L; H - 1 \rightarrow L\rangle - c.c.$ (0.0685)
III_x	4^1B_1	4.93	1.2645	$ H - 1 \rightarrow L + 1\rangle$ (0.8762) $ H \rightarrow L; H - 4 \rightarrow L + 1; H - 1 \rightarrow L + 4\rangle$ (0.0961)
$IV_{x\&y}$	9^1A_1	5.69	0.7967	$ H \rightarrow L + 2\rangle + c.c.$ (0.6138) $ H \rightarrow L + 2; H - 2 \rightarrow L; H - 2 \rightarrow L\rangle + c.c.$ (0.0735)
	7^1B_1	5.73	0.5869	$ H - 2 \rightarrow L + 1\rangle - c.c.$ (0.4428) $ H \rightarrow L + 3\rangle - c.c.$ (0.4169)
V_x	9^1B_1	6.07	0.3441	$ H \rightarrow L + 3\rangle - c.c.$ (0.4480) $ H - 2 \rightarrow L + 1\rangle$ (0.4168)
VI_y	13^1A_1	6.49	0.5088	$ H - 1 \rightarrow L + 3\rangle + c.c.$ (0.5910) $ H - 5 \rightarrow L\rangle - c.c.$ (0.1210)
VII_x	13^1B_1	6.74	0.4147	$ H - 2 \rightarrow L + 2\rangle$ (0.6083) $ H \rightarrow L; H \rightarrow L + 1\rangle - c.c.$ (0.2903)
$VIII_y$	19^1A_1	7.05	0.8317	$ H - 3 \rightarrow L + 2\rangle - c.c.$ (0.4896) $ H - 5 \rightarrow L\rangle - c.c.$ (0.2192)
IX_y	21^1A_1	7.29	0.5774	$ H - 5 \rightarrow L\rangle - c.c.$ (0.4025) $ H - 4 \rightarrow L + 2\rangle - c.c.$ (0.2637)
X_x	24^1B_1	7.89	0.3982	$ H - 4 \rightarrow L + 3\rangle + c.c.$ (0.3087) $ H \rightarrow L + 6\rangle + c.c.$ (0.2655)

Table S2. Excited states giving rise to peaks in the singlet linear absorption spectrum of phenanthrene, computed employing the FCI approach along with the standard parameters in the PPP model Hamiltonian.

Peak	State	E (eV)	Transition Dipole (\AA)	Dominant Contributing Configurations
D.F.	2^1A_1	3.35	0	$ H \rightarrow L + 1\rangle - c.c.$ (0.5841) $ H - 4 \rightarrow L\rangle - c.c.$ (0.1411)
I_x	1^1B_1	4.26	0.5925	$ H \rightarrow L\rangle$ (0.7891) $ H - 1 \rightarrow L + 1\rangle$ (0.4482)
$II_{x\&y}$	4^1A_1	5.15	0.7225	$ H - 1 \rightarrow L\rangle + c.c.$ (0.5233) $ H - 2 \rightarrow L\rangle + c.c.$ (0.2926)
	3^1B_1	5.24	1.5046	$ H - 1 \rightarrow L + 1\rangle$ (0.7582) $ H \rightarrow L\rangle$ (0.4236)
III_y	6^1A_1	5.59	0.6815	$ H - 2 \rightarrow L\rangle + c.c.$ (0.4418) $ H - 1 \rightarrow L + 3\rangle + c.c.$ (0.3183)
IV_x	6^1B_1	6.10	0.6860	$ H - 1 \rightarrow L + 2\rangle + c.c.$ (0.3758) $ H \rightarrow L + 3\rangle + c.c.$ (0.3694)
V_x	8^1B_1	6.40	0.6490	$ H \rightarrow L + 3\rangle + c.c.$ (0.4615) $ H - 1 \rightarrow L + 2\rangle + c.c.$ (0.3428)
$VI_{x\&y}$	11^1A_1	6.92	0.8429	$ H - 3 \rightarrow L + 1\rangle + c.c.$ (0.4894) $ H - 2 \rightarrow L\rangle + c.c.$ (0.3566)
	12^1B_1	7.01	0.4796	$ H - 2 \rightarrow L + 2\rangle$ (0.5146) $ H \rightarrow L; H - 1 \rightarrow L\rangle + c.c.$ (0.2966)
VII_y	17^1A_1	7.61	0.8929	$ H - 2 \rightarrow L + 3\rangle + c.c.$ (0.4433) $ H - 5 \rightarrow L\rangle + c.c.$ (0.3501)
$VIII_{x\&y}$	17^1B_1	7.92	0.2955	$ H - 1 \rightarrow L + 5\rangle + c.c.$ (0.4961) $ H - 3 \rightarrow L + 3\rangle$ (0.3290)
	20^1A_1	7.95	0.5256	$ H \rightarrow L + 5\rangle + c.c.$ (0.2192) $ H - 3 \rightarrow L + 2\rangle + c.c.$ (0.3894)
IX_x	22^1B_1	8.44	0.3042	$ H - 4 \rightarrow L + 3\rangle + c.c.$ (0.3847) $ H \rightarrow L; H - 5 \rightarrow L + 2\rangle - c.c.$ (0.2793)

Table S3. Excited states giving rise to peaks in the singlet linear absorption spectrum of chrysene, computed employing the QCI approach along with the screened parameters in the PPP model Hamiltonian.

Peak	State	E (eV)	Transition Dipole (\AA)	Dominant Contributing Configurations
D.F.	1^1B_u	3.11	0	$ H \rightarrow L + 1\rangle - c.c. (0.5658)$ $ H - 3 \rightarrow L + 2\rangle - c.c. (0.1241)$
I_{xy}	2^1B_u	3.86	1.2820	$ H \rightarrow L\rangle (0.8696)$ $ H - 1 \rightarrow L + 3; H \rightarrow L; H - 3 \rightarrow L + 1\rangle (0.0766)$
II_{xy}	3^1B_u	4.52	1.7260	$ H - 1 \rightarrow L\rangle + c.c. (0.6034)$ $ H - 1 \rightarrow L + 1\rangle (0.0943)$
III_{xy}	6^1B_u	5.09	1.2047	$ H - 1 \rightarrow L + 1\rangle (0.8551)$ $ H - 2 \rightarrow L + 2\rangle (0.0961)$
IV_{xy}	10^1B_u	5.81	0.4623	$ H - 2 \rightarrow L + 2\rangle (0.7226)$ $ H - 4 \rightarrow L\rangle - c.c. (0.2905)$
V_{xy}	11^1B_u	6.00	0.5548	$ H - 4 \rightarrow L\rangle - c.c. (0.5240)$ $ H - 2 \rightarrow L + 2\rangle (0.4171)$
VI_{xy}	16^1B_u	6.52	0.9847	$ H - 2 \rightarrow L + 3\rangle + c.c. (0.4430)$ $ H \rightarrow L + 6\rangle - c.c. (0.3047)$
VII_{xy}	18^1B_u	6.86	0.7404	$ H - 6 \rightarrow L\rangle - c.c. (0.4225)$ $ H - 4 \rightarrow L + 1\rangle - c.c. (0.2418)$
$VIII_{xy}$	25^1B_u	7.32	0.4887	$ H \rightarrow L; H \rightarrow L + 2\rangle + c.c. (0.3914)$ $ H - 2 \rightarrow L + 5\rangle - c.c. (0.2675)$
IX_{xy}	33^1B_u	7.67	0.7292	$ H - 4 \rightarrow L + 4\rangle (0.7372)$ $ H - 6 \rightarrow L + 1\rangle - c.c. (0.2196)$
X_{xy}	73^1B_u	9.17	0.2519	$ H - 5 \rightarrow L + 5\rangle (0.3179)$ $ H - 1 \rightarrow L + 1; H - 3 \rightarrow L\rangle + c.c. (0.2204)$

Table S4. Excited states giving rise to peaks in the singlet linear absorption spectrum of chrysenes, computed employing the QCI approach along with the standard parameters in the PPP model Hamiltonian.

Peak	State	E (eV)	Transition Dipole (\AA)	Dominant Contributing Configurations
D.F.	1^1B_u	3.33	0	$ H \rightarrow L + 1\rangle + c.c. (0.5783)$ $ H - 3 \rightarrow L + 2\rangle + c.c. (0.1720)$
I_{xy}	2^1B_u	3.96	0.9099	$ H \rightarrow L\rangle (0.8292)$ $ H - 1 \rightarrow L + 1\rangle (0.3102)$
II_{xy}	4^1B_u	5.08	1.8681	$ H \rightarrow L + 1\rangle - c.c. (0.5097)$ $ H - 1 \rightarrow L + 1\rangle (0.4207)$
III_{xy}	7^1B_u	5.76	0.7572	$ H - 4 \rightarrow L\rangle + c.c. (0.5074)$ $ H - 2 \rightarrow L + 2\rangle (0.4020)$
IV_{xy}	10^1B_u	6.38	0.7052	$ H - 2 \rightarrow L + 2\rangle (0.6623)$ $ H \rightarrow L + 4\rangle - c.c. (0.2435)$
V_{xy}	16^1B_u	7.17	0.9055	$ H - 2 \rightarrow L + 3\rangle - c.c. (0.3478)$ $ H - 3 \rightarrow L + 3\rangle (0.3264)$
VI_{xy}	18^1B_u	7.37	0.9251	$ H - 3 \rightarrow L + 3\rangle (0.3248)$ $ H - 2 \rightarrow L + 3\rangle - c.c. (0.3071)$
VII_{xy}	23^1B_u	7.77	0.4254	$ H \rightarrow L; H - 2 \rightarrow L + 1\rangle - c.c. (0.3096)$ $ H - 1 \rightarrow L; H - 2 \rightarrow L\rangle + c.c. (0.2059)$
$VIII_{xy}$	27^1B_u	8.02	0.7196	$ H - 3 \rightarrow L + 3\rangle (0.3120)$ $ H - 5 \rightarrow L + 2\rangle + c.c. (0.2905)$
IX_{xy}	31^1B_u	8.25	0.5931	$ H - 4 \rightarrow L + 4\rangle (0.5396)$ $ H - 3 \rightarrow L + 3\rangle (0.2552)$

Table S5. Excited states giving rise to peaks in the singlet linear absorption spectrum of picene, computed employing the QCI approach along with the screened parameters in the PPP model Hamiltonian.

Peak	State	E (eV)	Transition Dipole (Å)	Dominant Contributing Configurations
D.F.	2^1A_1	3.20	0	$ H \rightarrow L + 1\rangle - c.c.$ (0.5072) $ H \rightarrow L + 2\rangle - c.c.$ (0.2177)
I_x	1^1B_1	3.75	1.7007	$ H \rightarrow L\rangle$ (0.8521) $ H \rightarrow L; H - 3 \rightarrow L + 1; H - 1 \rightarrow L + 3\rangle$ (0.0651)
II_y	5^1A_1	4.54	1.0400	$ H \rightarrow L + 1\rangle + c.c.$ (0.6003) $ H - 1 \rightarrow L; H - 1 \rightarrow L\rangle - c.c.$ (0.0551)
$III_{x&y}$	4^1B_1	4.82	1.4373	$ H - 1 \rightarrow L + 1\rangle$ (0.8198) $ H - 1 \rightarrow L + 2\rangle + c.c.$ (0.1822)
	6^1A_1	4.93	0.5873	$ H - 2 \rightarrow L\rangle + c.c.$ (0.5937) $ H - 2 \rightarrow L + 3\rangle - c.c.$ (0.0629)
IV_x	7^1B_1	5.22	1.0175	$ H - 1 \rightarrow L + 2\rangle + c.c.$ (0.4406) $ H \rightarrow L + 3\rangle - c.c.$ (0.3649)
V_y	13^1A_1	5.74	0.4401	$ H - 3 \rightarrow L + 1\rangle - c.c.$ (0.5848) $ H \rightarrow L + 5\rangle - c.c.$ (0.0920)
VI_y	18^1A_1	6.10	0.2605	$ H - 2 \rightarrow L + 3\rangle - c.c.$ (0.4709) $ H \rightarrow L + 5\rangle - c.c.$ (0.2813)
VII_y	20^1A_1	6.30	0.4091	$ H - 5 \rightarrow L\rangle - c.c.$ (0.4288) $ H - 4 \rightarrow L + 1\rangle - c.c.$ (0.3685)
$VIII_y$	27^1A_1	6.63	1.0247	$ H - 2 \rightarrow L + 4\rangle - c.c.$ (0.4783) $ H \rightarrow L + 6\rangle - c.c.$ (0.2426)
IX_x	26^1B_1	6.93	0.4734	$ H - 3 \rightarrow L + 4\rangle + c.c.$ (0.4192) $ H - 1 \rightarrow L + 6\rangle - c.c.$ (0.2947)
X_x	30^1B_1	7.11	0.4116	$ H \rightarrow L; H - 2 \rightarrow L\rangle + c.c.$ (0.3626) $ H - 4 \rightarrow L + 3\rangle + c.c.$ (0.1620)
XI_y	40^1A_1	7.39	0.9253	$ H - 3 \rightarrow L + 5\rangle + c.c.$ (0.5120) $ H - 2 \rightarrow L + 7\rangle + c.c.$ (0.1536)
XII_y	52^1A_1	7.74	0.3322	$ H - 4 \rightarrow L + 5\rangle + c.c.$ (0.2751) $ H - 3 \rightarrow L + 6\rangle + c.c.$ (0.2615)

Table S6. Excited states giving rise to peaks in the singlet linear absorption spectrum of picene, computed employing the QCI approach along with the standard parameters in the PPP model Hamiltonian.

Peak	State	E (eV)	Transition Dipole (Å)	Dominant Contributing Configurations
D.F.	2^1A_1	3.33	0	$ H \rightarrow L + 1\rangle + c.c.$ (0.5280) $ H \rightarrow L + 2\rangle - c.c.$ (0.1878)
I_x	1^1B_1	3.88	1.1982	$ H \rightarrow L\rangle$ (0.8100) $ H - 1 \rightarrow L + 1\rangle$ (0.2910)
$II_{x&y}$	5^1A_1	4.67	0.4799	$ H \rightarrow L + 1\rangle - c.c.$ (0.4195) $ H - 2 \rightarrow L\rangle + c.c.$ (0.3711)
	4^1B_1	4.91	1.8167	$ H - 1 \rightarrow L + 1\rangle$ (0.7560) $ H \rightarrow L\rangle$ (0.2986)
III_y	6^1A_1	5.24	0.9225	$ H \rightarrow L + 1\rangle - c.c.$ (0.4077) $ H \rightarrow L + 2\rangle + c.c.$ (0.3760)
IV_x	6^1B_1	5.41	0.6892	$ H \rightarrow L + 3\rangle + c.c.$ (0.3891) $ H - 1 \rightarrow L + 2\rangle - c.c.$ (0.2760)
$V_{x&y}$	8^1B_1	5.76	0.6984	$ H - 2 \rightarrow L + 1\rangle - c.c.$ (0.4732) $ H - 2 \rightarrow L + 2\rangle$ (0.2833)
	10^1A_1	5.80	0.2939	$ H - 3 \rightarrow L + 1\rangle - c.c.$ (0.4509) $ H - 5 \rightarrow L\rangle - c.c.$ (0.2403)
VI_x	11^1B_1	6.18	0.6023	$ H - 2 \rightarrow L + 2\rangle$ (0.2833) $ H \rightarrow L + 4\rangle - c.c.$ (0.2136)
VII_y	19^1A_1	6.70	0.6771	$ H - 2 \rightarrow L + 4\rangle - c.c.$ (0.3927) $ H - 6 \rightarrow L\rangle - c.c.$ (0.2659)
$VIII_{x&y}$	$28A_1$	7.40	0.6738	$ H - 1 \rightarrow L + 7\rangle - c.c.$ (0.4362) $ H \rightarrow L + 1; H \rightarrow L + 1\rangle - c.c.$ (0.2439)
	27^1B_1	7.46	0.4659	$ H - 3 \rightarrow L + 4\rangle - c.c.$ (0.3566) $ H - 6 \rightarrow L + 1\rangle - c.c.$ (0.2359)
IX_y	36^1A_1	7.79	1.0850	$ H - 5 \rightarrow L + 3\rangle - c.c.$ (0.2918) $ H \rightarrow L + 1; H \rightarrow L + 1\rangle - c.c.$ (0.1880)
X_y	48^1A_1	8.26	0.3955	$ H \rightarrow L + 1; H - 2 \rightarrow L\rangle + c.c.$ (0.2294) $ H - 4 \rightarrow L + 5\rangle + c.c.$ (0.2239)

Table S7. Excited states giving rise to peaks in the singlet linear absorption spectrum of fulminene, computed employing the MRSDCI approach along with the screened parameters in the PPP model Hamiltonian.

Peak	State	E (eV)	Transition Dipole (\AA)	Dominant Contributing Configurations
D.F.	1^1B_u	2.86	0	$ H \rightarrow L + 1\rangle - c.c. (0.5642)$ $ H - 3 \rightarrow L + 2\rangle - c.c. (0.2027)$
I_{xy}	2^1B_u	3.34	1.7446	$ H \rightarrow L\rangle (0.8729)$ $ H \rightarrow L + 1\rangle + c.c. (0.0530)$
II_{xy}	4^1B_u	4.01	1.6754	$ H \rightarrow L + 1\rangle + c.c. (0.5903)$ $ H - 1 \rightarrow L + 1\rangle (0.1899)$
III_{xy}	6^1B_u	4.37	1.6424	$ H - 1 \rightarrow L + 1\rangle (0.8283)$ $ H \rightarrow L + 1\rangle + c.c. (0.1359)$
IV_{xy}	15^1B_u	5.39	0.9582	$ H - 3 \rightarrow L + 2\rangle + c.c. (0.5642)$ $ H - 1 \rightarrow L + 4\rangle + c.c. (0.2027)$
V_{xy}	23^1B_u	6.09	0.9477	$ H - 4 \rightarrow L + 4\rangle (0.4851)$ $ H - 3 \rightarrow L + 3\rangle (0.4434)$
VI_{xy}	38^1B_u	6.79	0.9639	$ H - 3 \rightarrow L + 5\rangle + c.c. (0.5146)$ $ H - 2 \rightarrow L + 8\rangle + c.c. (0.1993)$
VII_{xy}	42^1B_u	6.94	0.9091	$ H - 4 \rightarrow L + 6\rangle - c.c. (0.5326)$ $ H - 3 \rightarrow L + 5\rangle + c.c. (0.1373)$
$VIII_{xy}$	51^1B_u	7.28	0.6122	$ H - 5 \rightarrow L + 5\rangle (0.2875)$ $ H - 3 \rightarrow L + 8\rangle + c.c. (0.2258)$
IX_{xy}	77^1B_u	8.08	0.2669	$ H - 6 \rightarrow L + 8\rangle - c.c. (0.3798)$ $ H - 9 \rightarrow L + 3\rangle - c.c. (0.1741)$

Table S8. Excited states giving rise to peaks in the singlet linear absorption spectrum of fulminene, computed employing the MRSDCI approach along with the standard parameters in the PPP model Hamiltonian.

Peak	State	E (eV)	Transition Dipole (\AA)	Dominant Contributing Configurations
D.F.	1^1B_u	3.07	0	$ H \rightarrow L + 1\rangle + c.c. (0.5583)$ $ H - 3 \rightarrow L + 2\rangle - c.c. (0.1933)$
I_{xy}	2^1B_u	3.52	1.3412	$ H \rightarrow L\rangle (0.8026)$ $ H - 1 \rightarrow L + 1\rangle (0.2694)$
II_{xy}	5^1B_u	4.54	2.0679	$ H - 1 \rightarrow L + 1\rangle (0.6036)$ $ H \rightarrow L + 1\rangle - c.c. (0.3481)$
III_{xy}	6^1B_u	4.78	1.0719	$ H - 1 \rightarrow L + 1\rangle (0.4797)$ $ H \rightarrow L + 1\rangle - c.c. (0.3894)$
IV_{xy}	10^1B_u	5.59	0.7255	$ H - 2 \rightarrow L + 2\rangle (0.5363)$ $ H - 4 \rightarrow L\rangle - c.c. (0.2679)$
V_{xy}	12^1B_u	5.71	0.5968	$ H - 4 \rightarrow L + 1\rangle + c.c. (0.4299)$ $ H - 3 \rightarrow L + 2\rangle + c.c. (0.1960)$
VI_{xy}	15^1B_u	6.08	0.4820	$ H - 6 \rightarrow L\rangle + c.c. (0.4018)$ $ H - 2 \rightarrow L + 3\rangle + c.c. (0.2435)$
VII_{xy}	20^1B_u	6.51	0.8451	$ H - 2 \rightarrow L + 3\rangle + c.c. (0.3862)$ $ H - 7 \rightarrow L\rangle - c.c. (0.2441)$
$VIII_{xy}$	24^1B_u	6.94	0.6311	$ H - 4 \rightarrow L + 4\rangle (0.4070)$ $ H \rightarrow L; H - 1 \rightarrow L + 2\rangle + c.c. (0.2076)$
IX_{xy}	38^1B_u	7.51	1.2652	$ H - 4 \rightarrow L + 6\rangle - c.c. (0.2621)$ $ H - 5 \rightarrow L + 3\rangle - c.c. (0.2193)$
X_{xy}	47^1B_u	7.86	0.7282	$ H - 5 \rightarrow L + 3\rangle - c.c. (0.2738)$ $ H - 9 \rightarrow L + 2\rangle + c.c. (0.1910)$

Table S9. Excited states giving rise to peaks in the singlet linear absorption spectrum of [7]phenacene, computed employing the MRSDCI approach along with the screened parameters in the PPP model Hamiltonian.

Peak	State	E (eV)	Transition Dipole (Å)	Dominant Contributing Configurations
D.F.	2^1A_1	2.96	0	$ H \rightarrow L + 1\rangle + c.c. (0.4042)$ $ H \rightarrow L + 2\rangle - c.c. (0.3904)$
I_x	1^1B_1	3.34	2.1261	$ H \rightarrow L\rangle (0.8681)$ $ H - 2 \rightarrow L + 1\rangle - c.c. (0.0451)$
II_y	4^1A_1	3.88	0.7493	$ H - 1 \rightarrow L\rangle - c.c. (0.6046)$ $ H - 2 \rightarrow L\rangle + c.c. (0.0726)$
$III_{x\&y}$	6^1A_1	4.16	1.1036	$ H \rightarrow L + 2\rangle + c.c. (0.6003)$ $ H - 1 \rightarrow L\rangle - c.c. (0.0639)$
	4^1B_1	4.24	1.6175	$ H - 1 \rightarrow L + 1\rangle (0.6587)$ $ H - 1 \rightarrow L + 2\rangle - c.c. (0.3677)$
IV_x	6^1B_1	4.40	1.5693	$ H - 1 \rightarrow L + 1\rangle (0.5209)$ $ H - 2 \rightarrow L + 1\rangle - c.c. (0.4345)$
V_y	9^1A_1	4.79	0.5063	$ H - 1 \rightarrow L + 3\rangle - c.c. (0.5980)$ $ H - 3 \rightarrow L + 2\rangle + c.c. (0.0597)$
VI_y	16^1A_1	5.24	0.5600	$ H - 5 \rightarrow L\rangle + c.c. (0.4413)$ $ H - 4 \rightarrow L + 1\rangle + c.c. (0.2699)$
VII_y	19^1A_1	5.48	0.7462	$ H - 2 \rightarrow L + 4\rangle - c.c. (0.5669)$ $ H - 1 \rightarrow L + 4\rangle + c.c. (0.1905)$
$VIII_x$	24^1B_1	5.85	0.8260	$ H - 4 \rightarrow L + 3\rangle - c.c. (0.3825)$ $ H - 2 \rightarrow L + 5\rangle + c.c. (0.2944)$
IX_y	30^1A_1	6.19	0.2079	$ H - 3 \rightarrow L + 5\rangle + c.c. (0.4870)$ $ H - 7 \rightarrow L + 2\rangle - c.c. (0.1794)$
X_y	39^1A_1	6.51	0.1757	$ H \rightarrow L + 1; H - 2 \rightarrow L\rangle + c.c. (0.3221)$ $ H - 5 \rightarrow L + 4\rangle - c.c. (0.2550)$
XI_y	49^1A_1	6.85	0.5517	$ H - 2 \rightarrow L + 9\rangle + c.c. (0.3310)$ $ H - 4 \rightarrow L + 6\rangle - c.c. (0.3299)$
XII_y	59^1A_1	7.16	0.7976	$ H - 3 \rightarrow L + 8\rangle - c.c. (0.3916)$ $ H \rightarrow L + 2; H \rightarrow L + 2\rangle - c.c. (0.2117)$
$XIII_y$	68^1A_1	7.41	0.8776	$ H - 7 \rightarrow L + 5\rangle - c.c. (0.5621)$ $ H - 3 \rightarrow L + 8\rangle + c.c. (0.1321)$

Table S10. Excited states giving rise to peaks in the singlet linear absorption spectrum of [7]phenacene, computed employing the MRSDCI approach along with the standard parameters in the PPP model Hamiltonian.

Peak	State	E (eV)	Transition Dipole (\AA)	Dominant Contributing Configurations
D.F.	2^1A_1	3.31	0	$ H \rightarrow L + 1\rangle - c.c.$ (0.4320) $ H \rightarrow L + 2\rangle - c.c.$ (0.3321)
I_x	1^1B_1	3.68	1.6182	$ H \rightarrow L\rangle$ (0.7928) $ H - 1 \rightarrow L + 1\rangle$ (0.2598)
II_x	4^1B_1	4.67	2.0113	$ H - 1 \rightarrow L + 1\rangle$ (0.6059) $ H \rightarrow L\rangle$ (0.2720)
III_x	5^1B_1	4.85	1.2734	$ H - 2 \rightarrow L + 1\rangle + c.c.$ (0.3754) $ H \rightarrow L + 3\rangle - c.c.$ (0.3499)
IV_y	7^1A_1	5.03	1.0665	$ H - 2 \rightarrow L\rangle + c.c.$ (0.4111) $ H \rightarrow L + 1\rangle + c.c.$ (0.3830)
V_x	9^1B_1	5.53	0.7226	$ H - 2 \rightarrow L + 2\rangle$ (0.3797) $ H - 3 \rightarrow L\rangle - c.c.$ (0.3569)
VI_x	12^1B_1	5.82	0.6301	$ H \rightarrow L + 7\rangle + c.c.$ (0.2910) $ H - 3 \rightarrow L + 3\rangle$ (0.2861)
VII_y	17^1A_1	6.13	0.3527	$ H - 6 \rightarrow L\rangle + c.c.$ (0.2754) $ H - 3 \rightarrow L + 2\rangle - c.c.$ (0.2702)
$VIII_x$	$26B_1$	6.86	0.6935	$ H - 3 \rightarrow L + 2\rangle - c.c.$ (0.3139) $ H - 3 \rightarrow L + 3\rangle$ (0.2971)
IX_x	32^1B_1	7.36	0.4098	$ H - 4 \rightarrow L + 4\rangle$ (0.2364) $ H - 2 \rightarrow L + 5\rangle + c.c.$ (0.2236)
X_y	45^1A_1	7.62	0.8329	$ H - 3 \rightarrow L + 5\rangle - c.c.$ (0.2471) $ H - 2 \rightarrow L + 7\rangle + c.c.$ (0.2383)
$XI_{x\&y}$	51^1A_1	7.81	0.9191	$ H - 2 \rightarrow L; H - 1 \rightarrow L\rangle + c.c.$ (0.2214) $ H - 1 \rightarrow L + 1; H - 1 \rightarrow L + 2\rangle + c.c.$ (0.1569)
	47^1B_1	7.82	0.2754	$ H - 4 \rightarrow L + 10\rangle - c.c.$ (0.2035) $ H - 3 \rightarrow L + 9\rangle - c.c.$ (0.1882)
XII_y	59^1A_1	8.04	0.5942	$ H - 2 \rightarrow L + 9\rangle + c.c.$ (0.2214) $ H - 4 \rightarrow L + 8\rangle + c.c.$ (0.1927)
$XIII_{x\&y}$	59^1B_1	8.21	0.1863	$ H - 1 \rightarrow L; H - 1 \rightarrow L + 2\rangle + c.c.$ (0.2019) $ H - 6 \rightarrow L; H \rightarrow L\rangle + c.c.$ (0.1772)
	70^1A_1	8.29	0.6314	$ H - 6 \rightarrow L + 4\rangle + c.c.$ (0.1781) $ H - 7 \rightarrow L + 5\rangle + c.c.$ (0.1619)

Table S11. Excited states giving rise to peaks in the singlet linear absorption spectrum of [8]phenacene, computed employing the MRSDCI approach along with the screened parameters in the PPP model Hamiltonian.

Peak	State	E (eV)	Transition Dipole (\AA)	Dominant Contributing Configurations
D.F.	1^1B_u	2.84	0	$ H - 2 \rightarrow L\rangle + c.c. (0.5513)$ $ H - 1 \rightarrow L + 4\rangle + c.c. (0.1647)$
I_{xy}	2^1B_u	3.11	2.3654	$ H \rightarrow L\rangle (0.8595)$ $ H - 1 \rightarrow L + 1\rangle (0.0786)$
II_{xy}	5^1B_u	3.87	1.7035	$ H - 2 \rightarrow L\rangle - c.c. (0.5887)$ $ H - 2 \rightarrow L + 2\rangle (0.1627)$
III_{xy}	6^1B_u	4.08	2.0870	$ H - 1 \rightarrow L + 1\rangle (0.6179)$ $ H - 2 \rightarrow L + 2\rangle (0.4974)$
IV_{xy}	14^1B_u	4.85	0.9955	$ H - 1 \rightarrow L + 4\rangle - c.c. (0.4843)$ $ H - 2 \rightarrow L + 3\rangle - c.c. (0.2471)$
V_{xy}	16^1B_u	5.11	0.5581	$ H - 6 \rightarrow L\rangle - c.c. (0.5412)$ $ H - 4 \rightarrow L + 1\rangle - c.c. (0.1975)$
VI_{xy}	21^1B_u	5.41	0.6016	$ H - 4 \rightarrow L + 4\rangle (0.4106)$ $ H - 1 \rightarrow L + 5\rangle - c.c. (0.3323)$
VII_{xy}	32^1B_u	6.01	0.5398	$ H - 5 \rightarrow L + 4\rangle + c.c. (0.3636)$ $ H - 10 \rightarrow L\rangle + c.c. (0.2861)$
$VIII_{xy}$	41^1B_u	6.34	0.9425	$ H - 5 \rightarrow L + 5\rangle (0.3437)$ $ H - 3 \rightarrow L + 7\rangle - c.c. (0.3197)$
IX_{xy}	59^1B_u	6.89	0.2997	$ H - 6 \rightarrow L + 6\rangle (0.6732)$ $ H - 8 \rightarrow L + 4\rangle - c.c. (0.2568)$

Table S12. Excited states giving rise to peaks in the singlet linear absorption spectrum of [8]phenacene, computed employing the MRSDCI approach along with the standard parameters in the PPP model Hamiltonian.

Peak	State	E (eV)	Transition Dipole (\AA)	Dominant Contributing Configurations
D.F.	1^1B_u	3.13	0	$ H-2 \rightarrow L\rangle + c.c. (0.5307)$ $ H-1 \rightarrow L+4\rangle - c.c. (0.2166)$
I_{xy}	2^1B_u	3.41	1.8097	$ H \rightarrow L\rangle (0.7761)$ $ H-1 \rightarrow L+1\rangle (0.2679)$
II_{xy}	6^1B_u	4.48	2.1087	$ H-2 \rightarrow L+2\rangle (0.5421)$ $ H-1 \rightarrow L+1\rangle (0.3357)$
III_{xy}	7^1B_u	4.83	1.1518	$ H-2 \rightarrow L\rangle - c.c. (0.5209)$ $ H-2 \rightarrow L+2\rangle (0.1769)$
IV_{xy}	10^1B_u	5.31	0.8186	$ H-1 \rightarrow L+1\rangle (0.4928)$ $ H-5 \rightarrow L+1\rangle + c.c. (0.2471)$
V_{xy}	13^1B_u	5.56	0.5859	$ H-3 \rightarrow L+2\rangle + c.c. (0.4626)$ $ H-1 \rightarrow L+4\rangle + c.c. (0.1995)$
VI_{xy}	15^1B_u	5.78	0.4521	$ H \rightarrow L+6\rangle - c.c. (0.3747)$ $ H-4 \rightarrow L+1\rangle + c.c. (0.2556)$
VII_{xy}	20^1B_u	6.11	0.4880	$ H-4 \rightarrow L+4\rangle (0.2843)$ $ H-7 \rightarrow L\rangle + c.c. (0.2681)$
$VIII_{xy}$	24^1B_u	6.42	0.9346	$ H-3 \rightarrow L+3\rangle (0.3694)$ $ H-4 \rightarrow L+1\rangle + c.c. (0.2390)$
IX_{xy}	28^1B_u	6.67	0.5440	$ H-3 \rightarrow L+3\rangle (0.3096)$ $ H-7 \rightarrow L+3\rangle - c.c. (0.2249)$
X_{xy}	35^1B_u	6.95	0.3307	$ H \rightarrow L; H-1 \rightarrow L+2\rangle + c.c. (0.2572)$ $ H-2 \rightarrow L; H-1 \rightarrow L\rangle - c.c. (0.1810)$
XI_{xy}	46^1B_u	7.46	0.8000	$ H \rightarrow L; H-2 \rightarrow L+1\rangle + c.c. (0.3281)$ $ H-2 \rightarrow L+10\rangle - c.c. (0.1858)$
XII_{xy}	55^1B_u	7.70	0.9130	$ H \rightarrow L+12\rangle + c.c. (0.2608)$ $ H-9 \rightarrow L+2\rangle - c.c. (0.1819)$
$XIII_{xy}$	65^1B_u	8.00	0.6714	$ H-6 \rightarrow L+6\rangle (0.2055)$ $ H-12 \rightarrow L+2\rangle - c.c. (0.2007)$

Table S13. Excited states giving rise to peaks in the singlet linear absorption spectrum of [9]phenacene, computed employing the MRSDCI approach along with the screened parameters in the PPP model Hamiltonian.

Peak	State	E (eV)	Transition Dipole (Å)	Dominant Contributing Configurations
D.F.	2^1A_1	2.92	0	$ H - 2 \rightarrow L\rangle + c.c.$ (0.5012) $ H - 1 \rightarrow L\rangle - c.c.$ (0.2363)
I_x	1^1B_1	3.09	2.5945	$ H \rightarrow L\rangle$ (0.8565) $ H - 1 \rightarrow L + 1\rangle$ (0.1066)
II_y	4^1A_1	3.54	0.4135	$ H - 1 \rightarrow L\rangle + c.c.$ (0.6054) $ H \rightarrow L + 2\rangle - c.c.$ (0.0847)
$III_{x\&y}$	6^1A_1	3.93	1.4858	$ H \rightarrow L + 2\rangle - c.c.$ (0.6020) $ H - 1 \rightarrow L\rangle + c.c.$ (0.0819)
	5^1B_1	4.03	2.3516	$ H - 2 \rightarrow L + 2\rangle$ (0.4866) $ H - 2 \rightarrow L + 1\rangle - c.c.$ (0.4712)
IV_y	8^1A_1	4.38	0.5180	$ H - 1 \rightarrow L + 3\rangle - c.c.$ (0.5832) $ H \rightarrow L + 5\rangle - c.c.$ (0.1545)
$V_{x\&y}$	12^1B_1	4.79	0.3686	$ H - 3 \rightarrow L + 3\rangle$ (0.6435) $ H - 5 \rightarrow L + 1\rangle - c.c.$ (0.3833)
	15^1A_1	4.81	0.7933	$ H - 1 \rightarrow L + 4\rangle - c.c.$ (0.3961) $ H - 3 \rightarrow L + 2\rangle + c.c.$ (0.3058)
$VI_{x\&y}$	19^1A_1	5.07	0.5604	$ H - 6 \rightarrow L\rangle + c.c.$ (0.5404) $ H - 4 \rightarrow L + 1\rangle - c.c.$ (0.2207)
	18^1B_1	5.19	1.0923	$ H - 3 \rightarrow L + 4\rangle + c.c.$ (0.4564) $ H - 5 \rightarrow L + 2\rangle + c.c.$ (0.2418)
$VII_{x\&y}$	26^1B_1	5.66	0.2907	$ H - 9 \rightarrow L\rangle - c.c.$ (0.4075) $ H - 4 \rightarrow L + 4\rangle$ (0.3971)
	27^1A_1	5.67	0.6196	$ H - 1 \rightarrow L + 7\rangle - c.c.$ (0.3808) $ H \rightarrow L + 8\rangle + c.c.$ (0.2627)
$VIII_x$	29^1B_1	5.86	0.5180	$ H - 5 \rightarrow L + 5\rangle$ (0.4689) $ H - 3 \rightarrow L + 7\rangle$ (0.4018)
IX_y	34^1A_1	6.06	0.4973	$ H - 9 \rightarrow L + 1\rangle - c.c.$ (0.3837) $ H - 3 \rightarrow L + 6\rangle - c.c.$ (0.3130)
$X_{x\&y}$	40^1A_1	6.34	0.8060	$ H - 3 \rightarrow L + 8\rangle - c.c.$ (0.3787) $ H - 7 \rightarrow L + 5\rangle + c.c.$ (0.3593)
	37^1B_1	6.45	0.5350	$ H - 6 \rightarrow L + 5\rangle - c.c.$ (0.5396) $ H - 4 \rightarrow L + 7\rangle + c.c.$ (0.2330)
XI_y	49^1A_1	6.78	0.6662	$ H - 4 \rightarrow L + 8\rangle - c.c.$ (0.5761) $ H - 1 \rightarrow L + 12\rangle - c.c.$ (0.0844)

Table S14. Excited states giving rise to peaks in the singlet linear absorption spectrum of [9]phenacene, computed employing the MRSDCI approach along with the standard parameters in the PPP model Hamiltonian.

Peak	State	E (eV)	Transition Dipole (Å)	Dominant Contributing Configurations
D.F.	2^1A_1	3.29	0	$ H-2 \rightarrow L\rangle + c.c.$ (0.4580) $ H-1 \rightarrow L\rangle + c.c.$ (0.2550)
I_x	1^1B_1	3.46	2.0333	$ H \rightarrow L\rangle$ (0.7612) $ H-1 \rightarrow L+1\rangle$ (0.2845)
$II_{x&y}$	3^1A_1	3.94	0.2438	$ H-1 \rightarrow L\rangle - c.c.$ (0.4823) $ H-4 \rightarrow L+2\rangle + c.c.$ (0.2080)
	5^1B_1	4.49	2.7822	$ H-2 \rightarrow L+2\rangle$ (0.4861) $ H-1 \rightarrow L+2\rangle + c.c.$ (0.3834)
III_y	8^1A_1	5.00	1.1516	$ H \rightarrow L+2\rangle - c.c.$ (0.4766) $ H \rightarrow L+1\rangle - c.c.$ (0.2847)
$IV_{x&y}$	10^1A_1	5.29	0.4078	$ H-3 \rightarrow L+2\rangle - c.c.$ (0.3234) $ H-4 \rightarrow L+1\rangle + c.c.$ (0.2392)
	11^1B_1	5.33	0.8512	$ H-3 \rightarrow L+3\rangle$ (0.3860) $ H-3 \rightarrow L\rangle + c.c.$ (0.2949)
V_y	13^1A_1	5.72	0.4741	$ H-4 \rightarrow L+2\rangle + c.c.$ (0.3411) $ H-1 \rightarrow L+7\rangle + c.c.$ (0.2605)
VI_y	16^1A_1	5.90	0.3317	$ H-6 \rightarrow L\rangle - c.c.$ (0.3748) $ H-4 \rightarrow L+1\rangle + c.c.$ (0.2455)
VII_x	18^1B_1	6.10	0.2600	$ H-4 \rightarrow L+4\rangle$ (0.3439) $ H-6 \rightarrow L+2\rangle + c.c.$ (0.3067)
$VIII_{x&y}$	26^1B_1	6.52	0.7464	$ H-5 \rightarrow L+5\rangle$ (0.2853) $ H-7 \rightarrow L+7\rangle$ (0.2281)
	26^1A_1	6.58	0.6436	$ H-2 \rightarrow L+7\rangle + c.c.$ (0.2655) $ H-5 \rightarrow L+7\rangle - c.c.$ (0.2052)
$IX_{x&y}$	30^1A_1	6.88	0.4052	$ H-9 \rightarrow L+1\rangle - c.c.$ (0.2439) $ H-13 \rightarrow L\rangle + c.c.$ (0.2332)
	33^1B_1	7.01	0.2715	$ H-9 \rightarrow L\rangle + c.c.$ (0.2300) $ H-1 \rightarrow L+6\rangle + c.c.$ (0.1954)
$X_{x&y}$	43^1B_1	7.38	0.4384	$ H-5 \rightarrow L+6\rangle - c.c.$ (0.2448) $ H-7 \rightarrow L\rangle - c.c.$ (0.2351)
	42^1A_1	7.41	0.5450	$ H-11 \rightarrow L\rangle - c.c.$ (0.2639) $ H-7 \rightarrow L+5\rangle - c.c.$ (0.2150)
$XI_{x&y}$	47^1B_1	7.60	0.3654	$ H \rightarrow L+12\rangle - c.c.$ (0.2745) $ H-7 \rightarrow L+7\rangle$ (0.2376)
	50^1A_1	7.70	0.7497	$ H \rightarrow L+13\rangle + c.c.$ (0.2598) $ H-7 \rightarrow L+5\rangle - c.c.$ (0.1960)